Mariell Skaten

Experimental Investigation of the Total Performance of a Membrane Energy Exchanger

Master's thesis in Energy and Environment
Supervisor: Hans Martin Mathisen
Co-supervisor: Peng Liu

June 2021

Master's thesis

NTNU
Norwegian University of Science and Technology
Faculty of Engineering
Department of Energy and Process Engineering

NTNU
Kunnskap for en bedre verden

Mariell Skaten

Experimental Investigation of the Total Performance of a Membrane Energy Exchanger

Master's thesis in Energy and Environment
Supervisor: Hans Martin Mathisen
Co-supervisor: Peng Liu
June 2021

Norwegian University of Science and Technology
Faculty of Engineering
Department of Energy and Process Engineering

NTNU

Norwegian University of
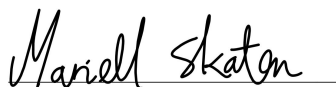Science and Technology

Preface

This master's thesis is a part of the research into membrane energy exchangers in cold climates at Norwegian University of Science and Technology (NTNU). It is closely connected to the research project *Defreeze MEE Now*, an industry-owned project by Flexit AS, and with SINTEF and NTNU as research partners. Earlier there have been several preliminary studies, master's theses and doctoral dissertations on the subject. This thesis is written during the spring semester of 2021 and accounts for 30 ETC. It is a continuation of the preliminary study from the fall of 2020.

I would like to thank my supervisor Prof. Hans Martin Mathisen and my co-supervisor Peng Liu, PhD. I am grateful for your guidance and advice throughout the thesis.

I am also grateful for the help I have received from Inge Havard Rekstad and Lars Konrad Sørensen from the EPT lab. You have helped me greatly with practical tasks and a practical understanding of the MEE test rig. Thanks also to Maria Justo-Alonso for letting me borrow your VOC sensors to conduct many of my experiments.

Lastly I would like to thank all my classmates at reading room B430 for your perseverance through this pandemic. Your motivational words at stressful times and company during lunch has been has been a paramount in the writing of this master's thesis.

Mariell Skaten

Trondheim, 11.06.2021

Abstract

Energy-efficient ventilation is crucial to reach today's strict Norwegian building regulations. Heat exchangers are therefore mandatory to install in ventilation systems to reduce the energy demand for ventilation. There are many types of heat exchangers that use different methods and designs to transfer heat. However, they all have one or more limitations. Membrane energy exchangers (MEE) try to solve problems concerning efficiency, frost, and cross-contamination using a membrane to separate the exhaust air and supply air. The exchanger can transfer both sensible and latent heat by making the membrane permeable to moisture. This increases efficiency and reduces the risk of freezing in the exhaust air channel. However, it brings up questions surrounding the ability of different contaminants to penetrate the membrane. This thesis aims to find the total performance of the MEE by experimentally investigating the potential transfer of volatile organic compounds (VOC) and odours through a porous polypropylene membrane, in addition to effectiveness and pressure drop.

Effectiveness and pressure drop are mainly influenced by the volumetric airflow rate and the thermodynamic properties of the ambient air. The transfer of contaminants depends on the physical properties of the membrane, which influences its selectivity. VOC and odour transfer is therefore evaluated through cross-contamination experiments on the MEE test rig using formaldehyde and household odour sources, respectively. The air leakage in the MEE core is also investigated in case the results are affected by internal or external leakages. After a literature study into odour measurements, it was decided to use the perceived air quality (PAQ) method to investigate the odour transfer through the membrane. An untrained sensory panel consisting of 19 people were set to evaluate the air acceptability (AA), odour intensity (OI) and hedonic tone (OI) after five different odour samples and two blank samples were inserted into the system.

Results from the experiments showed that the membrane achieved a high average sensible and latent effectiveness of 90% and 70%, respectively. The pressure drop through the MEE core is relatively high and increases when the volumetric airflow rate increases. However, measurements on formaldehyde transfer indicate that the crossover of contaminants decreases when the airflow rate is high. The crossover averages at 63% when the airflow rate is 7.3 L/s and has increased to 81.3% when the airflow rate is 4.2 L/s. Nonetheless, the crossover of formaldehyde is still relatively high. The odour experiment also indicates a large transfer through the membrane. When comparing the household odour samples to the blank samples there is a notable difference in air acceptability and odour intensity. Some odour samples were less noticeable due to differences in concentration caused by different volatility. However, the average odour intensity for the household odour samples was rated higher than the blank sample by 63% of the panel members for the first blank sample, and by 50% for the second blank sample.

The air leakage measurements using nitrous oxide (N_2O) indicate an internal leakage of 1.7% and an external leakage of 3.6%, which is relatively low. A plausible explanation for these contradicting measurements is that the membrane is less selective towards certain vapours and gases, like formaldehyde and odour.

The total performance of the polypropylene membrane is evaluated to be high in relation to heat transfer. However, the transfer of contaminants is larger than desired and could cause a reduction in indoor air quality. Future work should test additional membranes to verify the results and investigate measures that could reduce cross-contamination.

Sammendrag

Energieffektiv ventilasjon er avgjørende for å nå dagens strenge norske byggtekniske forskrifter. Varmevekslere er derfor obligatoriske å installere i ventilasjonsanlegg for å redusere energiforbruket til oppvarming. Det finnes mange typer varmevekslere som bruker ulike metoder og geometrisk design for å overføre varme. Problemet er at de fleste varmevekslere har en eller flere begrensninger. Membranvarmevekslere (MEE) prøver å løse problemer omkring lav effektivitet, frost og krysskontaminering ved hjelp av en membran som skiller avtrekksluft og tilluft. Varmeveksleren kan overføre både følbar og latent varme ved å gjøre membranen gjennomtrengelig for fuktighet. Dette øker effektiviteten og reduserer risikoen for at fukt i avtrekksluften fryser. Det forårsaker imidlertid spørsmål om hvorvidt urenheter i luften også er i stand til å trenge gjennom membranen. Denne masteroppgaven forsøker å finne den totale ytelsen til membranvarmeveksleren ved å eksperimentelt undersøke en mulig overføring av flyktige organiske forbindelser (VOC) og lukt gjennom en porøs polypropylenmembran, i tillegg til å undersøke effektivitet og trykkfall.

Effektivitet og trykkfall påvirkes hovedsakelig av den volumetriske luftstrømningshastigheten og luftens fysiske tilstand. Overføringen av urenheter avhenger av de fysiske egenskapene til membranen, som igjen påvirker dens selektivitet. VOC og luktoverføring evalueres derfor gjennom krysskontaminasjonseksperimenter på MEE-testriggen ved bruk av henholdsvis formaldehyd og lukt som vanligvis finnes i husholdninger. Luftlekkasjen i varmevekslerkjernen undersøkes også i tilfelle resultatene påvirkes av interne eller eksterne lekkasjer. Etter en litteraturstudie på utførelsen av luktmålinger ble det besluttet å bruke opplevd luftkvalitet metoden (Percieved Air quality - PAQ) for å undersøke luktoverføringen gjennom membranen. Et utrent sensorisk panel bestående av 19 personer ble satt for å evaluere luftakseptabilitet, luktintensitet og hedonisk tone etter at fem forskjellige luktprøver og to blindprøver ble tilført systemet.

Resultat fra eksperimentene viste at membranen oppnådde en høy gjennomsnittlig følbar og latent effektivitet på henholdsvis 90% og 70%. Trykkfallet gjennom varmevekslerkjernen er relativt høyt og øker når den volumetriske luftstrømmen øker. Målinger indikerer imidlertid at krysskontamineringen av formaldehyd avtar når luftstrømningshastigheten er høy. Gjennomsnittsverdien er 63% når lufthastigheten er 7,3 L/s og har økt til 81,3% når lufthastigheten synker til 4,2 L/s. Likevel er krysskontamineringen av formaldehyd fortsatt relativt høy. Lukteksperimentet indikerer også at det er krysskontaminering gjennom membranen. Når man sammenligner luktprøvene med blindprøvene, er det en merkbar forskjell i luftakseptabilitet og luktintensitet. Noen luktprøver var mindre merkbare på grunn av forskjeller i konsentrasjon forårsaket av ulik flyktighet. Likevel ble den gjennomsnittlige luktintensiteten ble vurdert til å være høyere enn den første blindprøven av 63% av panelmedlemmene, og av 50% for den andre blindprøven.

Luftlekkasjemålingene ble utført ved hjelp av dinitrogenoksid (N_2O) og indikerer en intern lekkasje på 1,7% og en ekstern lekkasje på 3,6%. Dette tilsier at lekkasjen er relativt lav. En mulig forklaring på disse motstridende målingene er at membranen er mindre selektiv mot visse gasser, som formaldehyd og lukt.

Den totale ytelsen til polypropylenmembranen vurderes å være høy når det kommer til varmeoverføring. Imidlertid er overføringen av forurensninger høyere enn ønsket og kan føre til en reduksjon i inneluftkvaliteten. Fremtidig forskning bør fokusere på å teste flere membraner for å verifisere resultatene. Det bør også undersøkes om det finnes tiltak som kan redusere krysskontaminering.

Table of Contents

G Odour Samples

V

List of Figures

List of Tables

List of Nomenclature

Abbreviations

AA   Air Acceptability

ASHRAE   The American Society of Heating, Refrigerating and Air-Conditioning Engineers

COPD   Chronic obstructive pulmonary disease

EATR   Exhaust Air Transfer Ratio

HT   Hedonic Tone

IAQ   Indoor Air Quality

ISO   International Organization for Standardization

MEE   Membrane energy exchanger

NTU   Number of Transfer Units

OACF   Outdoor Air Correction Factor

OI   Odour Intensity

OT   Odour detection Threshold

PAQ   Perceived Air Quality

PD   Percentage of Dissatisfied

SBS   Sick Building Syndrome

TVOC   Total Volatile Organic Compound

VOC   Volatile Organic Compound

WHO   World Health Organization

Greek letters

α Thermal diffusivity $[m^2/s]$ or Probability of error [%]

δ Thickness $[mm]$

ϵ Effectiveness $[-]$

λ Thermal conductivity $[W/mK]$

ν Kinematic viscosity $[m^2/s]$

ρ Density $[kg/m^3]$

σ	Ratio of cross-sectional area $[-]$

Parameters

$\dot{m}$	Mass Flow Rate $[kg/s]$
a_r	Aspect ratio $[-]$
C	Concentration $[mol/m^3]$
c_p	Specific Heat Capacity $[J/kgK]$
D	Diffusivity $[m^2/s]$
D_h	Hydraulic diameter [m]
f	Darcy friction factor $[-]$
h	Convective heat transfer coefficient $[W/m^2K]$
J	Flux $[m^3(STP)/m^2s]$
j	Chilton-Colburn j factor $[-]$
k	Convective moisture transfer coefficient $[m/s]$
K_L	Loss coefficient $[-]$
$K_{c/e}$	Contraction/expansion coefficient $[-]$
Le	Lewis number $[-]$
Nu	Nusselt number $[-]$
P	Pressure $[Pa]$, or permeability $[mol/m^2sPa]$
p	Partial pressure $[Pa]$
P/ℓ	Permeance $[mol/m^2SPa]$
Pr	Prandtl number $[-]$
Q	Gas flow rate $[m^3/s$ or $L/min]$
R	Gas constant $[8.314J/molK]$
r	Moisture resistance $[m^2s/kg]$
Re	Reynolds number $[-]$
s	Standard deviation $[-]$
Sc	Schmidt number $[-]$
Sh	Sherwood number $[-]$
St	Stanton number $[-]$
t	Temperature $[K]$
u	Velocity of the fluid $[m/s]$
W	Moisture content $[kg/kg]$
A	Area $[m^2]$
D	Diameter $[m]$
L	Length $[m]$

R	Ratio for heat/mass capacity $[-]$
U	Heat Transfer Coefficient $[W/m^2 K]$
V	Velocity $[m/s]$

Sub- and superscripts

i	Species or inlet
o	Outlet
avg	Average
e	Exhaust
L	Latent heat
m	Moisture or membrane
max	Maximum
min	Minimum
n	Number
p	Porous
S	Sensible or supply
tot	Total
v	Water

Chapter 1

Introduction

1.1 Background

The average European spends 90% of their time indoors, with 2/3 of it being in their homes (Sarigiannis 2014). It is therefore important to ensure a good indoor environment. Poor indoor air quality can significantly affect human health. Some common health effects are eye, nose, and throat irritation, respiratory diseases, allergic reactions, and in extreme cases it can lead to cancer (Attramadal, Schwarze, and Becher 2015). The reality is that the volatile organic compound (VOC) concentration can be 2 to 5 times higher indoors than outdoors. VOCs are chemical particles emitted from gases, solids or liquids, and can be found in many common household items (US EPA 2018). Other factors like light, noise, and odour can also affect the human perception of the indoor environment. If the source of the poor indoor environment is hard to determine, we often use the umbrella term *sick building syndrome* (Mentese et al. 2020).

Poor technical solutions in ventilation system seem to be a recurring character for buildings where the inhabitants have a negative experience of the indoor environment (Attramadal, Schwarze, and Becher 2015). The ventilation system needs to supply the building with fresh air at a sufficient airflow rate based on the appropriate building regulations. Norwegian regulations also state that the ventilation system should have a heat recovery efficiency of 80% from the exhaust to the supply air (DiBK 2017).

This can only be achieved with the use of heat exchangers. There are several types of heat exchangers, but the similarity is that they transfer heat between two or more fluids. The heat transfer can happen directly or indirectly, between the same phases or different phases, in different flow patterns, and the design can look very different. Some of the most common designs are tubular-, plate- and rotary heat exchangers (Cengel and Cimbala 2014). A weakness for some of these heat exchangers is that they experience cross-contamination between the supply and exhaust air. This is only a problem for air-to-air exchangers where the supply and exhaust are in contact with each other, like in rotary exchangers (Patel et al. 2013). To reduce cross-contamination, membranes are often used to separate the air flows. Membranes can transfer both heat and moisture, meaning the exchanger can utilise both the sensible and latent heat of the airflow. This leads to an increase in efficiency for the system (Niu and L. Zhang 2001). The idea of membrane energy exchangers (MEE) as we know them today were first presented in an article by Zhang in 1999 (L. Zhang and Jiang 1999). The problem occurs when the membrane is unable to prevent the transfer of contaminants. A high VOC transfer will reduce the indoor air quality. The membrane may also transfer odour, annoying the occupants further. Choosing the correct membrane and exchanger type is therefore crucial.

1.2 Objectives and Research Questions

The aim of this thesis is to evaluate the total performance of the membrane in the membrane energy exchanger. In order to achieve this the following tasks are considered:

- Conduct a state of the art literature study on membrane energy exchangers and experiments on VOC- and odour transfer.
- Collect background theory on relevant subjects needed to perform measurements and analyse results.
- Construct new membrane energy exchanger cores with the appropriate techniques to facilitate the testing of additional membranes.
- Investigate and compare the cross contamination in the membrane energy exchanger by testing the transfer of VOCs, odour and air leakage through the membranes.

By investigating these topics, the following research questions will be answered:

1. Is the perceived air quality method the best method for conducting odour experiments?

2. Has the odour experiment been influenced by the background odour in the test rig?

3. Are the membranes equally selective to different vapours and gases?

4. What is the total performance of the membrane?

1.3 Scope and Limitations

This thesis will use the knowledge acquired in the preliminary study to investigate MEEs further. The focus area will be porous membrane materials. Dense membranes were the norm in membrane energy exchangers for a long time. In recent years porous membranes have been investigated because they have shown excellent heat transfer properties. However, there are some questions surrounding the membranes ability to stop contaminant transfer through the pores. Therefore, the scope of this thesis will be to experimentally investigate the contaminant transfer through the membrane to investigate the potential cross-contamination. By combining the results from experiments on effectiveness, pressure drop and cross-contamination, the total performance of the MEE will be assessed.

The initial plan was to investigate three different porous membrane materials. The membrane currently installed in the test rig is made out of polypropylene, and SINTEF and Flexit AS provided two additional membrane materials. In order to investigate the two new membranes, new exchanger cores would have to be constructed. Unfortunately, these plans had to be changed due to unforeseen circumstances at the lab. The production of polycarbonate parts was delayed several times due to mechanical problems with the water jet cutter. In the end, one of the membranes where constructed. The use of the lab also had to be coordinated with SINTEF, who needed access to the environmental chamber to conduct their own research. This caused further delays, which meant two new membranes were never installed and tested at the MEE test rig.

The scope of the thesis had to be scaled down because only one membrane was tested instead of three. Initially, the plan was to compare the three porous membranes and investigate if there was a connection between the total performance and the membrane's physical parameters. The new scope focuses on testing additional contaminants to examine the cross-contamination through the polypropylene membrane more extensively.

1.4 Report Structure

The thesis is structured into nine chapters. This chapter, Chapter 1, presents background information about ventilation systems and the issues this technology tries to solve. The aim of the thesis is then presented by the objectives and research questions and constricted in scope and limitations.

- Chapter 2 presents the most recent and relevant literature in the field. This includes a study into odour analysis techniques and an investigation of how extensive the problem of contaminant and odour transfer in ventilation systems is. Lastly a state of the art literature review on porous membrane materials is conducted to keep up with the latest developments.

- Chapter 3 presents relevant theoretical information about MEEs, volatile organic compounds and odour.

- Chapter 4 presents the layout of the MEE test rig and construction method of the exchanger core. Two different layouts are described; one used to investigate the physical performance of the MEE, and one used to conduct the contaminant experiments using formaldehyde, odour and tracer gas.

- Chapter 5 presents the method on how all the experiments are conducted. This includes sensible and latent effectiveness, pressure drop, odour transfer, VOC transfer and testing of the air leakage through the MEE core.

- Chapter 6 presents the results from all the experiments conducted on the test rig.

- Chapter 7 presents the discussion of the results, possible sources of error and relates the different findings to each other in order to answer the research questions.

Finally, the conclusion is presented in chapter 8 and proposal for future work in chapter 9. References and appendices follow immediately after.

Chapter 2

Literature Study

Li-Zhi Zhang has from 1999 published several research papers about heat and mass transfer in membrane-based exchangers. In the years following, other researchers have also started to investigate the applications of MEEs. There is continuous progress in the field, which is published in different scientific journals. This literature study focuses on progress made in the field of odour and VOC transfer in MEEs and on membrane materials. The literature is mainly from the last five years; however, some older articles have also been included if there are few recent publications on the topic. Some of the research articles were also mentioned in the preliminary study.

2.1   Odour Analysis Techniques

Odour analysis techniques can be divided into three main groups; sensorial, instrumental and mathematical. The optimal odour measurement technique will vary in different situations and which parameters are most important for the research. To get a comprehensive view of the situation, multiple techniques can be combined in an integrated approach (Bax, Sironi, and Capell 2020). Table 2.1 shows an overview of the most common techniques in odour analysis.

Table 2.1: Odour analysis techniques. Based on (Bax, Sironi, and Capell 2020)

Sensorial	Dynamic olfactometry (EN 13725:2003)
	Field inspection (EN 16481:2016)
	Field Olfactometry
	Citizen science
Instrumental	Electronic nose
	Chemical analysis
	Gas chromatography (GC)
Mathematical	Dispersion models
	Odour emission factors
	Emission databases

Sensory analysis is a scientific discipline used to assess the surrounding environment using one or several senses (Lewkowska et al. 2016). Dynamic olfactometry and field inspection are standardised sensory odour measurement methods according to European level (EN 13725:2003 and EN 16841:2016, respectively). Both methods rely on a trained panel to evaluate the presence of odours. Dynamic olfactometry measures the odour concentration expressed in European odour units per cubic meter (ou_E/m^3). The concentration is increased until the odour detection threshold (OT) is met. Field inspection is used for odour characterisation in a defined area and does not give any information about the concentration. The human nose has a higher sensitivity than electronic instruments but cannot always distinguish between different odours. Sensorial techniques are also affected by subjective interpretations of the odour. Therefore the results may not be as repeatable and reliable as instrumental techniques.

Instrumental techniques use an analytical device to identify and quantify an odorous substance. Some of the most common instrumental odour analysis techniques are listed in table 2.1. Electronic noses are instruments designed to mimic the human olfactory organ. They analyse the odour sample as a whole like the human nose would do. However, they can deliver continuous results and eliminate the human error factor (Bax, Sironi, and Capell 2020). Chemical analysis is used when a full investigation of the chemical compounds in the odour sample is required. Gas Chromatography (GC) is a technique used to separate and analyse samples by differences in boiling point, vapour pressure or polarity (Stauffer, Dolan, and Newman 2008). GC is often combined with mass spectrometry (GC-MS) or olfactometry (GC-O). Mass spectrometry allows for detailed identification and quantification of the odorous substance. GC-O combines the instrumental analysis of the odour with human olfaction to determine the presence, quality, and intensity of the odour (Bax, Sironi, and Capell 2020). Figure 2.1 shows how the odour sample is supplied and then separated in the column before it is divided into two equal streams. One stream goes to an olfactometry port, where a trained panellist assesses the odour, while the second stream travels to a mass spectrometer detector to be analysed.
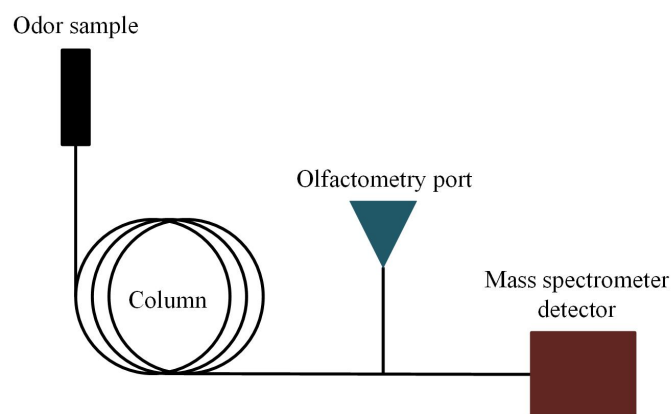

Figure 2.1: Gas Chromatography - Olfactometry. Based on (Bax, Sironi, and Capell 2020).

Mathematical odour analysis techniques use models and databases to predict how odour disperses in an environment and the resulting concentration. This method is not relevant for the thesis and therefore not researched as thoroughly.

2.2   Odour Sources in Membranes

Odorous compounds are found in many volatile chemical species like sulphur, nitrogen and VOC (Conti, Guarino, and Bacenetti 2020). A prevalent concentration of these substances causes an unpleasant sensory experience. The VOC concentration in a building is often one of many factors affecting indoor air quality (IAQ). Inside ventilation systems, the air supply filter is the main source of odours. This is the systems first contact point with the outside air, and dust can start to build up (Hyttinen et al. 2007). Ventilation ducts and heat exchangers may emit some odour if the supply air filter does not catch all contaminants in the outdoor air or the system experiences cross-contamination between the supply and exhaust channel. Huizing et al. (2015) conducted a study on contaminant transport in MEEs where they tested five different membranes and compared their crossover rates and selectivity. The results showed a crossover rate of between 0.01% and 15% for the membranes. Even though 15% crossover is considered moderate, the authors conclude that it is expected that the contaminants would have a minimal impact on the IAQ under standard conditions. It is possible to increase the air change rate to compensate for the crossover rate. However, this will reduce the energy efficiency and increase ventilation costs (Huizing, Chen, and Wong 2015).

Šenitková and Kraus (2018) conducted a study investigating the emissions and odours emitted from common indoor materials and appliances. The emissions were analysed by gas chromatography, and the odours by an untrained panel rating the odour intensity (OI) and air acceptability (AA). The study indicates that the human nose is more sensitive to odours than the measurement device. However, the human nose may give an unsatisfactory result if the samples are below the odour threshold or mixed with other VOCs. Combining the sensory analysis with a chemical analysis will provide a more comprehensive understanding of the indoor air. Chemical analysis can also identify potential health effects caused by the pollutants in the air. Three different indoor materials were investigated, and the tests showed that the polyamide carpet, painted gypsum board and wallpaper emitted 0.170 mg/m^2h, 0.190 mg/m^2h and 0.043 mg/m^2h of TVOC, respectively. Based on the chemical analysis, all the materials are classified as low polluting. However, the percentage of dissatisfied people were relatively high for the materials; 56% for the polyamide carpet, 56% for the painted gypsum board, and 88% for the wallpaper. The limit of materials to be classified as low polluting is 15% (Senitkova and Kraus 2018). Both the research study from Huizing, Chen, and Wong (2015) and Šenitková and Kraus (2018) show the importance of conducting sensory analyses in addition to instrumental measurements.

2.3   Suitable Membrane Materials

Dense membranes have been the most common type of membrane in MEEs for a long time, but more and more researchers are starting to investigate the advantages of porous membranes (Woods 2014) (Rashidi et al. 2019). Switching to a porous material can improve the heat transfer in exchangers because they have a large contact surface and change the boundary layer thickness. This helps increase both the conductive and convective heat transfer. Properties like thickness, thermal conductivity, porosity, and the material structure can influence the result (ibid.).

In the last few years, Ahmed K. Albdoor and his associates have conducted several research studies on the performance of porous membrane materials. Albdoor, Ma and Cooper (2019) investigated five different porous membranes, where two of them were of the same material but had different pore size. The research showed that the membrane with the smaller pore size had the highest moisture diffusion resistance. At a relative humidity of 30%, the moisture diffusion resistance for the PVDF membrane changed from 48.7

to 63.1 m^2s/kg when the pore size decreased from 0.45 to 0.22 μm. The high moisture diffusion resistance of the PVDF22 membrane also manifests itself in the effectiveness. The latent effectiveness is 67% for the PVDF45 membrane and 1.2% lower, at 65.8%, for the PVDF22 membrane when the humidity was at 45%.

In an article published in 2020, the same researchers conducted further experiments on the five membrane materials. They evaluated the water contact angle, moisture diffusivity and elastic modulus for each membrane. Figure 2.2 shows the findings. A water contact angle below 90° indicates that the membrane is hydrophilic. The moisture diffusivity specifies the transfer capacity of moisture through the membrane and affects the latent effectiveness. Elastic modulus describes how an object reacts to being deformed due to stress, and a low elastic modulus has been related to poor performance in MEEs (Albdoor, Ma, and Cooper 2020). Based on the measurements, the PVDF45 membrane performed the best.

Table 2.2: Comparison of physical properties of five porous membranes (Albdoor, Ma, and Cooper 2019) (Albdoor, Ma, and Cooper 2020)

Material	Pore size [μm]	Water contact angle [°]	Moisture diffusivity [m/s]	Elastic modulus [Pa]
Nylon10	0.1	41.4	1.41×10^{-6}	5.16×10^{8}
Nylon45	0.45	40.5	1.50×10^{-6}	1.89×10^{8}
PES10	0.1	52.3	1.57×10^{-6}	7.67×10^{7}
PVDF22	0.22	76.2	1.59×10^{-6}	5.20×10^{8}
PVDF45	0.45	74.4	1.91×10^{-6}	4.97×10^{8}

Albdoor et al. (2021) investigated the improved water vapour transport properties of polymeric membranes by adding a thin layer of metal-organic frameworks (MOFs). MOFs have been shown to increase the permeability and surface hydrophilicity of membranes in previous studies conducted on membranes used for filtration and water distillation (Albdoor, Ma, Cooper, et al. 2021). The surface hydrophilicity describes the membranes ability to attract water molecules. This is an essential property since most porous membranes are hydrophobic, meaning they do not absorb or desorb water molecules (Liu et al. 2016).

In the study, two different MOF particles (ZIF-8 and HKUST-1) were tested in an air-to-air MEE. At pristine conditions, the porosity of the membrane was measured to be 72.4%. After the coating was applied, the porosity increased to 80.6% and 86.1% for the ZIF-8 and HKUST-1 coating, respectively. The surface hydrophilicity is measured by the water contact angle (WCA). The WCA dropped from 74.4° to 58.3° for the ZIF-8 coating and to 44.9° for the HKUST-1 coating. A lower water contact angle means the membrane transports moisture easily through the membrane. The experiments show that the moisture content and temperature of the air had minimal effects on the performance of the MEE. This implies that the MOF particles are not affected by outdoor air conditions and could be used on membranes in hot and cold climates (Albdoor, Ma, Cooper, et al. 2021).

3 Chapter

Theory

This chapter presents relevant theory about the subjects investigated in this thesis. The theory comes from recognised research, national and international standards and technical textbooks. Subchapter 3.1.1 and 3.1.2 where originally written in conjunction with the preliminary study and are presented again in this thesis with some minor changes.

3.1 Membrane Energy Exchanger

Membrane energy exchangers (MEE) are equipped with a water-permeable membrane so that both heat and moisture can be transferred between the supply air and exhaust air. The exchanger can now utilise the sensible and latent heat in the air, increasing the total effectiveness.

In summer conditions, the exhaust air absorbs heat and moisture from the supply air, which cools and dehumidifies the incoming air. In winter conditions, the excess heat and humidity is recovered from the exhaust air and reduces the total energy need for ventilation while also decreasing the frosting limit of the unit. Frost formation occurs when the exhaust air temperature drops below the dew point temperature, and moisture in the air begins to freeze. The consequence is blockage of the air channels, which causes a reduction in the exchanger effectiveness. In total energy exchangers, the exhaust air temperature and the humidity ratio decrease at the same time. This decreases the dew point temperature and allows the exhaust air to reach temperatures below zero before frosting is detected (Rafati Nasr et al. 2014). Membrane energy exchangers are also helpful in preventing microbes and bacteria from transferring between air streams. The pores in the membrane are small enough to stop unwanted particles from passing (Woods 2014).

Cross-flow exchangers have long been the dominant flow arrangement due to the simplicity of duct sealing. However, the effectiveness is 10% lower than for counter-flow arrangements. The only problem with pure-counter flow arrangement is creating a tight seal between the supply and exhaust air ducts (L. Zhang 2014). Research from 2010 found that quasi-counter flow heat exchangers had a 5% increase in sensible and latent effectiveness compared to cross-flow arrangements (L. Zhang 2010). A quasi-counter flow exchanger consists of a counter-flow core with a cross-flow heater. This arrangement utilises the high effectiveness of the counter-flow exchanger and the simple sealing of the cross-flow exchanger (Kays and London 1984). Figure 3.1 shows the three mentioned flow arrangement.
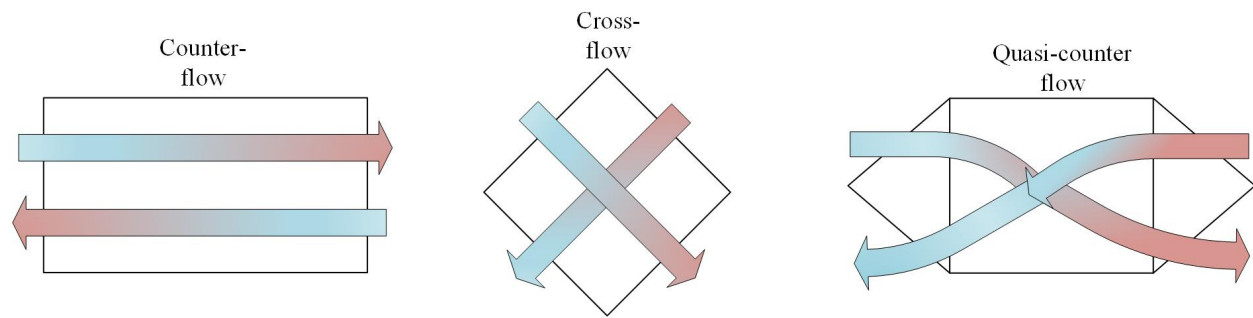
Figure 3.1: Different heat exchanger arrangements

The energy-saving of MEEs relates to the sensible and latent effectiveness and the energy consumption for fans. The effectiveness depends on the flow rate per membrane area. Because of membrane moisture resistance, the latent effectiveness is always lower than the sensible effectiveness. The membrane moisture resistance varies with temperature and humidity and therefore fluctuates depending on the season and location. Sensible effectiveness stays unaffected by these variations but could be slightly influenced by the membrane conductivity (Woods 2014). Choosing the suitable membrane for the system is therefore very important.

A membranes function is an MEE is to create a barrier between two different air conditions. The membrane performance depends on the thickness, diffusivity (for porous membranes) or permeability (for dense membranes), density, porosity, thermal conductivity and selectivity of the membrane (Liu et al. 2016). Dense membranes are commonly in the order of 0.1 nm, and porous membranes are in the order of 0.1 μm. Dense membranes are the most common type for MEEs (Woods 2014). Transportation through dense membranes happen by adsorption and desorption because of the small pore size, and it is preferable to use thin membranes to reduce the diffusion path length. Ideal dense membranes for use in total energy exchangers should also have a high water vapour permeance and at the same time be selective over other gases and vOCs. These properties make them almost impermeable to odours (Liu et al. 2017). Porous membranes have been investigated for use in MEEs in later years. These membranes are hydrophobic, meaning the material repels water. It creates a liquid/gas interface on the surface of the membrane. In order to transfer the liquid, the surface tension has to break by applying air pressure. This process is called diffusion (Woods 2014). With their large pores, porous membranes have a large contact surface, enabling it to increase the heat transfer between fluids (Rashidi et al. 2019).
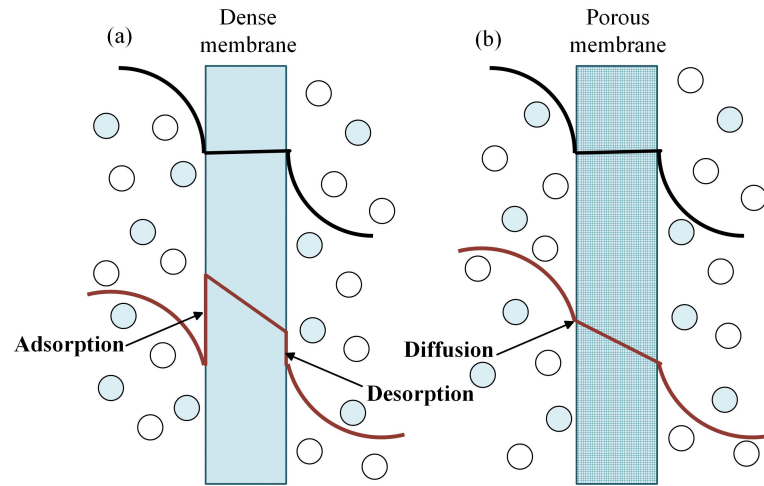
Figure 3.2: Dense and porous moisture transfer through the membrane (a) Dense membrane and (b) Porous membrane. Based on (Liu et al. 2017)

Flat-sheet membranes are not stable enough to support themselves. Therefore, spacers are necessary to ensure that they do not collapse or stick together (L. Zhang 2008). Spacers also help increase the heat and mass transfer on the air-side boundary layer. The disadvantage is that the spacers also increase the pressure drop in the channel (Woods 2014). Consequently, the geometric design of the spacers is essential to limit the pressure drop (Koester et al. 2016). Table 3.1 shows a comparison of the effectiveness and pressure drop in common air-to-air heat and/or energy exchangers.

Table 3.1: Comparison of the effectiveness and pressure drop in common air-to-air heat and/or energy exchangers. Based on (ASHRAE 2016).

	Fixed Plate	MEE	Energy Wheel	Heat Wheel	Heat Pipe	Rund-around Coil
Sensible ϵ [%]	50-75	55-75	65-80	65-80	40-60	45-65
Latent ϵ [%]	-	25-60	50-80	-	-	-
Pressure drop [Pa]	100-1000	100-500	125-2500	125-2500	0-250	0

3.1.1 The Effectiveness-NTU Method

The Effectiveness-NTU Method is used to find the correlation between heat and mass transfer in an energy exchanger and the system's geometry, design, and operating conditions. The effectiveness is related to the Number of Transfer Units (NTU). However, the NTU method only assesses the sensible heat, while the Effectiveness-NTU method evaluates both sensible and latent heat (L. Zhang 2014).

Number of Transfer Units

The number of transfer units is a dimensionless parameter used to evaluate the performance of a heat exchanger. In sensible-only heat exchangers, the sensible NTU number is calculated based on the heat exchangers total transfer area, A, the total heat/moisture transfer coefficient (U), heat capacity, C_p, and

fluid flow rate, $\dot{m}$ (L. Zhang 2008). The fluid with the lowest flow rate, and therefore also lowest heat capacity, is used in the calculations. MEEs transfer both heat and mass; therefore, the latent NTU number must also be calculated. Here the calculations are based on the density of the fluid, ρ, instead of thermal capacity because latent heat does not affect the temperature of the fluid. Equations 3.1 and 3.2 show how the NTU numbers are calculated.

$$NTU_S = \frac{A_{tot}U_S}{(\dot{m}C_p)_{min}} \tag{3.1}$$

$$NTU_L = \frac{A_{tot}U_L}{(\dot{m})_{min}} \tag{3.2}$$

Sensible Heat Transfer Coefficient

The total heat transfer coefficient for sensible heat, U_S (eq. 3.3), is based on the convective heat transfer coefficient, h, and the heat conduction through the membrane, δ/λ_m. In reality, the heat conduction is negligible due to how thin the membrane is (L. Zhang 2012).

$$U_S = \left(\frac{1}{h_s} + \frac{\delta}{\lambda_m} + \frac{1}{h_e}\right)^{-1} \tag{3.3}$$

The convective heat transfer coefficient, h, is based on the Nusselt number, Nu, the thermal conductivity of the air, λ_a, and the hydraulic diameter, D_h (Liu et al. 2016) (L. Zhang 2012). In this form, the convective heat transfer coefficient equation (eq. 3.4) represents a heat exchanger with no spacers. To correct for the presence of spacers, the Chilton-Colburn j factor for heat (eq. 3.5) is added to the convective heat transfer coefficient (L. Zhang 2014) (Liu et al. 2017). St is the Stanton number which can also be written as a function of the Nusselt number, Nu, the Reynolds number (eq. 3.16), and the Prandtl number, Pr.

$$h = \frac{Nu\lambda_a}{D_h} \tag{3.4}$$

$$j_h = St_h Pr^{2/3} = \frac{Nu}{RePr^{1/3}} \tag{3.5}$$

The Nusselt number is defined as the ratio of conduction heat transfer to convection heat transfer in a fluid under the same conditions. For a rectangular channel, the Nusselt number can be calculated with equation 3.6 which is based on the aspect ratio, a_r (eq. 3.7). The aspect ratio is the channel height divided by the channel width (Siegele and Ochs 2019).

$$Nu = -7.4814 \cdot a_r^3 + 18.535 \cdot a_r^2 - 15.663 \cdot a_r + 8.235 = 8.235 \tag{3.6}$$

$$a_r = \frac{height}{width} \tag{3.7}$$

Latent Heat Transfer Coefficient

The latent heat transfer coefficient, U_L, is based on the convective moisture transfer coefficient, k, and the moisture resistance of the membrane, r_{mm} (Liu et al. 2016). Contrary to the sensible heat transfer coefficient, the membrane properties are quite important. The convective moisture resistance contributes to between 50 and 63% of the total moisture resistance. The resistance is dependent on outdoor temperatures and humidities and will reduce with higher outdoor humidity and lower outdoor temperature (Min and Su 2011). Equation 3.8 shows how the latent heat transfer coefficient is calculated.

$$U_L = \left(\frac{1}{k_s} + r_{mm} + \frac{1}{k_e} \right)^{-1} \tag{3.8}$$

For a porous membrane, the moisture resistance (eq. 3.9) is dependent on the thickness of the membrane, δ, and the diffusivity, D_p.

$$r_{mm} = \frac{\delta}{1.65 \times 10^5 D_p} \tag{3.9}$$

The convective moisture transfer coefficient (eq. 3.10) can be found using the Sherwood number, Sh, the water vapour diffusion coefficient, D_v, and the hydraulic diameter, D_h. The equation is only applicable to exchangers with no spacers without adding the Chilton-Colburn j factor for moisture (eq. 3.11).

$$k = \frac{Sh D_v}{D_h} \tag{3.10}$$

$$j_m = St_m Sc^{2/3} = \frac{Sh}{Re Sc^{1/3}} \tag{3.11}$$

The Sherwood number is used when calculating the convective moisture transfer coefficient (eq. 3.12). It is defined as the ratio of convective mass transfer to diffusive mass transport in a fluid. The Sherwood number is also dependent on the Nusselt number and the Lewis number (eq. 3.15) (L. Zhang 2012).

$$Sh = Nu Le^{-1/2} \tag{3.12}$$

The Prandtl number, Pr, Schmidt number, Sc, and Lewis number, Le, are three dimensionless numbers defined by equation 3.13, 3.14 and 3.15, respectively. The numbers are all material properties and not dependent on the fluid flow. The Prandtl number defines the correlation between the viscosity, ν, and the thermal conductivity, α, of a fluid. Fluids with a low Pr-number are good for heat conduction because they flow easily and have a high thermal conductivity. The Schmidt number puts the fluid's viscosity in connection with the diffusion coefficient, D_{va}. The Lewis number describes the correlation between mass diffusion and thermal conductivity. It can also be calculated by dividing the Prandtl number on the Schmidt number (Rapp 2017).

$$Pr = \frac{\nu}{\alpha} \qquad (3.13) \qquad\qquad Sc = \frac{\nu}{D_{va}} \qquad (3.14) \qquad\qquad Le = \frac{D_{va}}{\alpha} = \frac{Pr}{Sc} \qquad (3.15)$$

The Reynolds number, Re, is a dimensionless number that relates the internal forces to the viscous forces in the fluid. It can be used to classify the flow in a pipe, i.e. laminar ($Re \ll 2000$) or turbulent flow ($Re \gg 2000$) (L. Zhang 2008). Laminar flow is characterised as smooth flow without swirling, or *eddies*, in the flow. If the flow rate or viscosity increases enough, eddies will start to form, and the flow is considered turbulent. Equation 3.16 shows the formula for the Reynolds number. It uses the velocity of the fluid, u, the hydraulic diameter and the kinematic viscosity to determine the correct number (L. Zhang 2010).

$$Re = \frac{uD_h}{\nu} \tag{3.16}$$

Effectiveness

The sensible and latent effectiveness must be calculated for both the cross-flow section (eq. 3.17) and the counter-flow section (eq. 3.18) (L. Zhang 2008). The difference between sensible and latent effectiveness is which NTU-number is used, S/L.

$$\epsilon_{S/L} = 1 - exp\left[\frac{exp(-NTU_{S/L}{}^{0.78}) - 1}{NTU_{S/L}{}^{-0.22}}\right] \tag{3.17}$$

$$\epsilon_{S/L} = \frac{NTU_{S/L}}{1 + NTU_{S/L}} \tag{3.18}$$

Kays et al. (1968) came up with a numerical solution for the sensible effectiveness in a quasi-counter flow heat exchanger. The effectiveness is based on the NTU numbers for the cross-flow and counter-flow section in the exchanger. Table 3.2 shows the relationship between the effectiveness and NTU numbers. It shows that the effectiveness of the quasi-counter flow heat exchanger increases with the number of transfer units. It is also apparent that the cross-flow NTU has the most influence on effectiveness.

Table 3.2: Sensible effectiveness as a function of NTU for the counter-flow and cross-flow part of the heat exchanger (Kays, Jain, and Sabherwal 1968)

		$NTU_{cross-flow}$							
		0	1	2	3	4	5	6	7
	0	0	0.476	0.615	0.682	0.723	0.752	0.773	0.790
	1	0.500	0.649	0.714	0.751	0.777	0.795	0.810	0.821
	2	0.667	0.739	0.775	0.798	0.815	0.828	0.838	0.846
$NTU_{counter-flow}$	3	0.750	0.792	0.816	0.831	0.843	0.852	0.860	0.866
	4	0.800	0.828	0.844	0.855	0.863	0.870	0.876	0.880
	5	0.834	0.853	0.865	0.873	0.880	0.885	0.889	0.893
	6	0.856	0.872	0.881	0.887	0.892	0.897	0.900	0.903
	7	0.875	0.886	0.893	0.899	0.903	0.906	0.909	0.912

3.1.2 Pressure Drop

Heat exchangers work by forcing the exhaust and inlet fluid close to each other to exchange thermal energy. The driving force for this exchange is pressure difference mainly caused by fans, pumps or compressors in the system. A large pressure drop also affects the saturation temperature in the exchanger and therefore also affects the heat transfer rate (Shah and Sekulic 2003).

When calculating the pressure drop, we usually use the symbol Δ to indicate that the drop is calculated over a designated area. The pressure drop is not uniform throughout the heat exchanger. Therefore, it is common to calculate the total pressure drop as a sum of major and minor losses, like shown in equation 3.19 (Cengel and Cimbala 2014).

$$\Delta P_{total} = \Delta P_{major} + \Delta P_{minor} \tag{3.19}$$

Equation 3.20 and figure 3.3 shows the pressure drop at different locations through the exchanger. 1,2,3 and 4 represents the upstream, entrance, exit, and downstream, respectively.

$$\Delta P = \Delta P_{1-2} + \Delta P_{2-3} - \Delta P_{3-4} \tag{3.20}$$
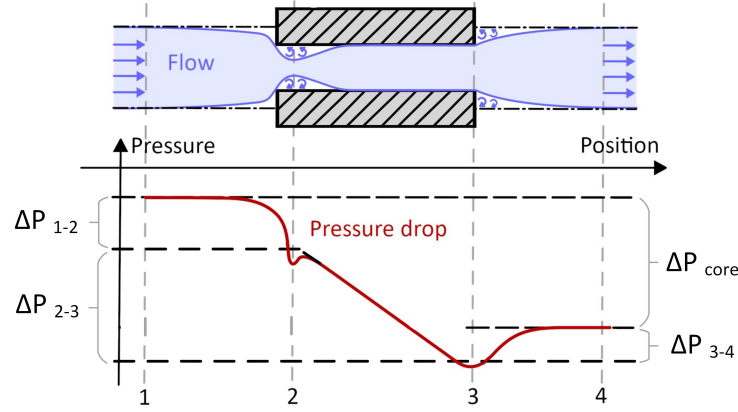
Figure 3.3: Pressure drop of air stream moving through a heat exchanger. Based on (Lecomte-Saur 2020) and (Shah and Sekulic 2003)

Major Losses

Major losses in a heat exchanger are considered a sum of losses in the core and conjunction with fluid distribution in the headers, ducts and diffusers (Shah and Sekulic 2003). The core pressure drop should be dominant because this creates a uniform flow distribution in the heat exchanger. The general equation for the major pressure losses is presented in equation 3.21.

$$\Delta P_{major} = \sum_i f_i \frac{L_i}{D_i} \frac{\rho V^2{}_i}{2} \tag{3.21}$$

i represents pipe sections with the same diameter

Where f is the Darcy friction factor, L/D relates to the length and diameter of the pipe or duct, and $\rho V^2/2$ is the dynamic pressure. The formula assumes steady-state and isothermal flow and a constant friction factor along the flow length.

For a circular pipe with laminar flow, the Darcy friction factor, f (eq. 3.22), can also be written as a function of the Reynolds Number. It shows that for laminar flows (Re $\ll 2000$), the friction factor is independent of the pipe roughness (Cengel and Cimbala 2014).

$$f = \frac{64\mu}{\rho D V^2{}_{avg}} = \frac{64}{Re} \tag{3.22}$$

Minor Losses

Minor losses are caused by components interrupting the fluid flow, like bends, valves, inlets and outlets. These losses are small compared to the major losses in the core but are essential to include because of the flow separation and mixing they cause (ibid.). Equation 3.23 shows the general presentation of pressure drop due to minor losses.

$$\Delta P_{minor} = \sum_j K_{L,j} \frac{\rho V^2{}_j}{2} \tag{3.23}$$

j represents components that cause minor losses (bends, entrance, exit)

K_L is the loss coefficient. It can be determined experimentally, with the manufacturer's values or by standards organisations like ASHRAE. This method is quite uncertain because it does not consider the roughness, diameter or Reynolds Number. The entrance and exit pressure drop can be expressed more specifically with the ratio of the channel cross-sectional area to the frontal area, σ (eq. 3.24) (Cengel and Cimbala 2014).

$$\sigma = \frac{A_2}{A_1} = \frac{A_3}{A_4} \tag{3.24}$$

Equation 3.25 and 3.26 shows the full formulas for entrance and exit pressure drop, respectively. Both the contraction coefficient, K_c, and the expansion coefficient, K_e, are functions of σ and can be found with the help of the Reynolds number and cross-sectional geometry.

$$P_i = (1 - \sigma_i^2 + K_c) \frac{\rho V^2{}_i}{2} \tag{3.25}$$

$$P_e = (1 - \sigma_e^2 - K_e) \frac{\rho V^2{}_e}{2} \tag{3.26}$$

3.2 Volatile Organic Compounds

Volatile Organic Compounds (VOC) are chemicals emitted from gases, solids or liquids that evaporate quickly at room temperature (Anand, Philip, and Mehendale 2014). The volatility of the compounds is related to their boiling point, where a low boiling point related to high volatility. Table 3.3 shows the three most common classifications of organic compounds; very volatile, volatile and semi-volatile.

Table 3.3: Classification of organic compounds based on their boiling point (US EPA 2014)

	Boiling point [$^\circ C$]	
	Start	**End**
Very volatile organic compounds (VVOC)	<0	50-100
Volatile organic compounds (VOC)	50-100	240-260
Semi volatile organic compounds (SVOC)	240-260	380-400

Studies show that the VOC concentration can be 2 to 5 times higher indoors than outdoor (US EPA 2018). The indoor sources are divided into stationary and variable sources. The stationary sources are related to degassing from paint, building materials and furnishings, and the contribution will be relatively stable over time. The variable sources are related to human activities like using cleanings products, smoking

and cooking. These sources are present in smaller time intervals. Most outdoor volatile organic compounds come from exhaust emissions from cars. These contaminants can enter the building through windows, openings and the ventilation system, contributing to the total VOC level. The term total VOC (TVOC) is often used to describe the total concentration of different organic compounds in an environment.

There is no official upper limit for TVOC concentration in buildings in Norway. The Norwegian Institute of Public Health (NIPH/FHI) states that a quantified limit would be an inefficient indicator of indoor air quality. TVOC measurements can consist of significantly different VOC compositions and therefore give no information on the effects of individual substances and interaction between substances. However, TVOC is an indicator of the pollution level in the air (Attramadal, Schwarze, and Becher 2015). The standard NS-EN 15251:2007 proposes some limit values for defining *Low* and *Very Low* polluting buildings. Table 3.4 shows the upper limit value for TVOC and some common VOCs and odour dissatisfaction.

Table 3.4: The definition of very low and low polluting buildings, according to EN 15251:2007.

	Low polluting	Very low polluting
TVOC [mg/m^2h]	0.2	0.1
Formaldehyde [mg/m^2h]	0.05	0.02
Carcinogenic compounds (IARC) [mg/m^2h]	0.005	0.002
Odour dissatisfaction [%]	15	10

3.2.1 Health Effects

Some volatile organic compounds have known negative health effect in humans when they are inhaled. The problems usually occur after long term exposure at high concentrations, but less serious problems have also been reported at lower concentrations. The water solubility of the VOC determines which organs are at risk for exposure. Compounds with a high water solubility are quickly absorbed in the mucous membrane and will not travel far down the airways. These VOCs usually cause problems in the mucous membranes in the eyes, nose and throat area. Compounds with low water solubility can move further down the airways towards the lungs. Deposition of particles and fibres in this area can be quite serious as they disappear quite slowly, giving them more time to cause damage (ibid.). Some common health problems attributed to VOCs are:

- Eye, nose and throat irritation
- Respiratory diseases and allergic reactions in the respiratory tract (allergy, asthma, COPD)
- Cancer

The International Agency for Research on Cancer (IARC) is an agency under WHO which specialises in cancer research. They have classified substances into four groups by their carcinogenic potential in humans. Table 3.5 shows the different groups and their definition and gives an example some common VOCs in the respective groups.

Table 3.5: Classification of carcinogenic substances, based on (WHO 2011).

Group	Classification	Source
1	Carcinogenic to humans	Benzene, Formaldehyde
2A	Probably carcinogenic to humans	Tetrachloroethylene, Methylene chloride
2B	Possibly carcinogenic to humans	Acetaldehyde
C	Not classifiable as to its carcinogenicity to humans	Toluene, Xylene

3.2.2 Formaldehyde

Formaldehyde is a colourless, flammable and highly reactive gas. Table 3.6 shows some of the chemical properties of formaldehyde ($HCHO$). Exposure to formaldehyde has been linked to several health problems, and it is a regulated substance under the Norwegian Labour Inspection Authority (Attramadal, Schwarze, and Becher 2015). Formaldehyde is produced in natural processes like biomass combustion and decomposition or anthropogenic activities, including the combustion of fuels and the manufacturing of resins and preservatives. Indoor sources of formaldehyde are usually due to human activities like cooking, fireplace or candle burning, smoking, cleaning and using electronic devices. It is also emitted from new building materials like particle boards, insulation, resins, glue, lacquers, paints, wallpapers and textiles (WHO 2010). The release of formaldehyde from new materials can last for several months, depending on the temperature and humidity level indoors (Attramadal, Schwarze, and Becher 2015).

Table 3.6: Formaldehyde properties, from PubChem and Wikipedia

	Molecular Weight [g/mol]	Boiling Point [$°C$]	Density [kg/m^3]
Formaldehyde, $HCHO$	30.026	-19.1	815

Short term exposure to formaldehyde may irritate the mucous membranes in the eyes, nose and throat C It can lead to concentration problems, sneezing, coughing, tearing, nausea, difficulty breathing and odour discomfort. Odour discomfort occurs at concentrations from 50 $\mu g/m^3$ and up to 500 $\mu g/m^3$, and the smell is described as pickle-like and quite strong (ibid.). Several epidemiological studies have shown that long term exposure to formaldehyde at high concentration can cause cancer in humans. IARC has stated that there is enough evidence to prove that formaldehyde causes sinonasal cancer and myeloid leukaemia. It is therefore classified as a level 1 carcinogenic (WHO 2011). There are also some indications that long term exposure can lead to the development or worsening of asthma in children. However, there are some uncertainties in this correlation due to weaknesses with the clinical study design. Due to these health risks, the Norwegian Labour Inspection Authority has defined a limit of exposure to formaldehyde to 100 $\mu g/m^3$ for up to 30 minutes (Attramadal, Schwarze, and Becher 2015).

3.2.3 Crossover of Contaminants

Crossover is usually caused by contaminants transferring from the exhaust air to the supply air with the help of a rotary wheel or static pressure differences between the air streams. The latter is a potential problem for MEEs. The crossover of contaminants in MEEs can be calculated using different methods. One method looks

at leakages in the system, indicating there could be an exchange of contaminants. This can be calculated with the Exhaust Air Transfer Ratio (EATR). EATR is the ratio of concentration increase between the supply and exhaust air. The formula is given in equation 3.27 and is based on the airborne contaminant concentration, C. The contaminant concentration is usually given in parts per million (PPM) (Patel et al. 2013). In an ideal system with no leakages, the EATR ratio would be zero..

$$EATR = \frac{C_{s,out} - C_{s,in}}{C_{e,in} - C_{s,in}} \tag{3.27}$$

Figure 3.4 illustrates how contaminants from the exhaust air inlet ($C_{e,in}$) can transfer through the membrane of a counter-flow exchanger and into the supply air stream.
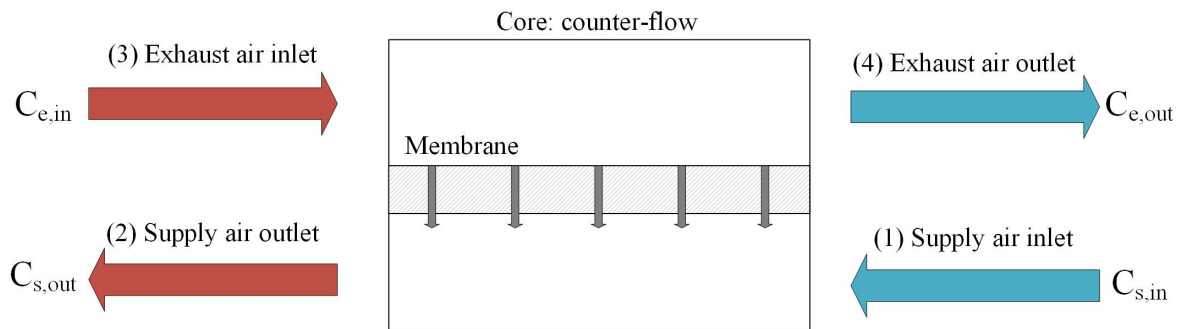
Figure 3.4: Air and potential VOC transfer in the core of a membrane energy exchanger

Table 3.7 shows a comparison of the EATR for some common air-to-air heat and/or energy exchangers (ASHRAE 2016). When comparing the ratio to the effectiveness (see table **??**) it is evident that the exchangers which transfer both sensible and latent heat, or include rotating parts, have the highest exhaust air transfer ratio.

Table 3.7: Comparison of the EATR and OACF ratio in common air-to-air heat and/or energy exchangers. Based on (ASHRAE 2016).

	Fixed Plate	MEE	Energy Wheel	Heat Wheel	Heat Pipe	Run-around Coil
EATR [%]	0-2	0-5	0.5-10	0.5-10	0-1	0

Another method that assesses the transfer properties of the membrane looks at the crossover, χ, flux, J, and permeance, P/ℓ, of the membrane (Huizing, Chen, and Wong 2015). The crossover ratio is the transfer of contaminants, C, from the exhaust to the supply air. It is calculated based on the percentage increase of a species, i. Flux is defined as the flow rate of the species transferred through a membrane with the area, A. It also uses the gas flow rate, Q, partial pressure, p, molar volume, V_m, gas constant, R, and temperature to calculate the flux. The permeance expresses the species ability to penetrate the membrane and is based on the flux and the partial pressure between the exhaust inlet and supply outlet. The formulas are shown in equation 3.28, 3.29 and 3.30, respectively.

$$\chi_i = \frac{C_{i,s,out}}{C_{i,e,in}} * 100\% \tag{3.28}$$

$$J_i = \frac{Q_2 p_{i,2} V_m}{RT\,A} \tag{3.29}$$

$$\frac{P_i}{\ell} = \frac{J_i}{p_{i,3} - p_{i,2}} \tag{3.30}$$

Membranes can be more selective towards one chemical compound compared to another. Equation 3.31 shows how the permeability of one compound can be compared to the total permeability of the system to find the selectivity, α. Water vapour (H_2O) is used as an example as it is an important parameter in efficient energy exchangers (Huizing, Chen, and Wong 2015).

$$\alpha_{H_2O/i} = \frac{P_{H_2O}}{P_i} \tag{3.31}$$

3.2.4   Air Leakage

Air leakage between internal and external parts of the membrane energy exchanger can cause a reduced efficiency and increased crossover of contaminants. Types of air leakage in heat exchangers vary with the type and design but are defined as unwanted air entering or exiting the supply or exhaust air stream. Air leakages can lead to an increased pressure drop in the system, affecting the effectiveness and the energy use for fans in the system. Leakage between the supply and exhaust air can cause significant problems with the air quality. The EATR ratio (eq. 3.27) gives an indication of the internal leakage in the exchanger. However, air leakage is usually investigated with the help of a pressurisation test or tracer gas test (NS 2011). Only the tracer gas method will be presented in this subchapter.
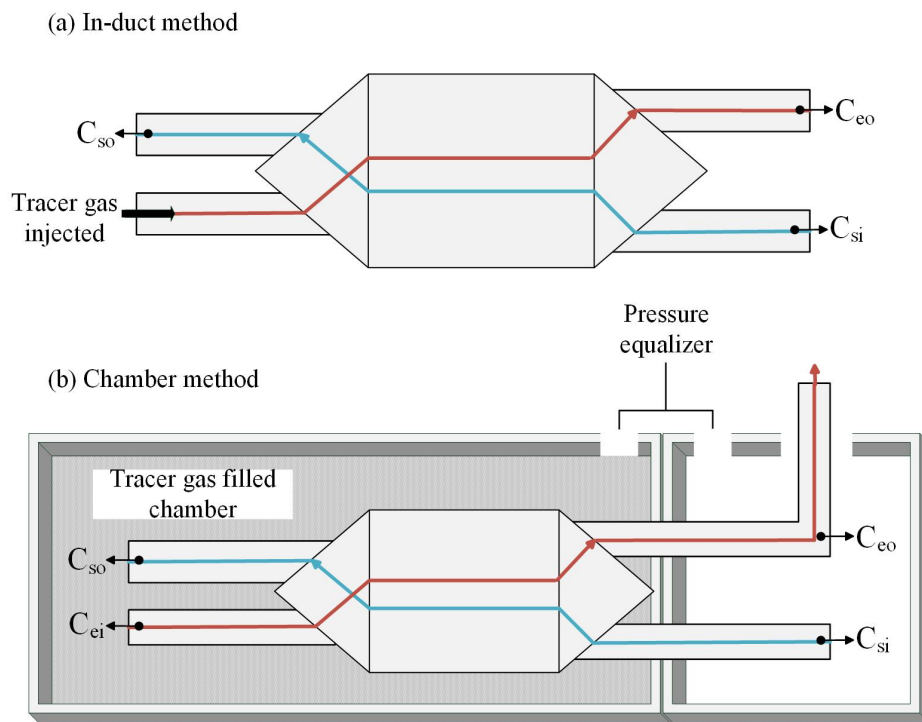

Figure 3.5: (a) In-duct method and (b) chamber method for dispersing and measuring tracer gas

There are two possible test configurations to chose from when conducting a tracer gas test; either the in-duct method or the chamber method. Figure 3.5 shows how the tracer gas is dispersed, and where the measuring points are.

The in-duct method can be used on exchangers with negligible casing leakage. Tracer gas is injected at the supply air inlet side, and the gas concentration is measured at three other entry or exit points of the exchanger. This method calculates the internal leakage. The chamber method, as the name indicates, in conducted by placing the supply and exhaust part of the heat exchanger into two different chambers. Tracer gas is inserted at a high concentration on the exhaust air inlet side. The concentration is later measured on the supply air outlet side, and gives the total air leakage of the exchanger. The leakage is calculated with the recirculation fraction, R, given in equation 3.32. R is the fraction of air recirculated from the exhaust to the supply air due to internal and/or external leakages. C_i is the tracer gas concentration.

$$R = \frac{1}{n} \sum_{i=n}^{n} \left[\frac{c_{so,i} - c_{si,i}}{c_{ei,i} - c_{si,i}} \right] \tag{3.32}$$

When choosing a tracer gas to use in the air leakage measurements, some factors must be considered. Problems could then arise if there is a chemical reaction between the gases at one or more locations in the test rig. They could also experience decomposition over time as they pass through the membrane. This might impact the readings from the measurement device as the gas does not behave identically throughout the test rig (Sherman n.d.). Therefore, tracer gasses are usually inert, i.e. a gas that does not chemically react with other gases under a set of given conditions. Some of the most common tracer gases are nitrous oxide (N_2O), sulphur hexafluoride (SF_6), hexafluorobenzene (C_6F_6) and carbon dioxide (CO_2) (Laussmann and Helm 2011). Table 3.8 shows some properties of the mentioned tracer gases.

Table 3.8: Tracer gas properties, from PubChem and Wikipedia

	Molecular Weight [g/mol]	Boiling Point [$^\circ C$]	Density [kg/m^3]
Nitrous oxide, N_2O	44.013	-88.5	1220
Sulphur hexafluoride, SF_6	146.06	-63.8	6.17
Hexafluorobenzene, C_6F_6	186.05	80.2	1610
Carbon dioxide, CO_2	44.009	-78.48	1.98

3.3   Odour

According to the International Organization for Standardization (ISO 5492:2008), odour is defined as an organoleptic attribute from certain VOCs detected by the olfactory organ. The stimulation of the olfactory organ triggers a sensation of odour (Conti, Guarino, and Bacenetti 2020).

Odour intensity and odour concentration are the most important descriptors of an odour (Lewkowska et al. 2016). Odour intensity often uses the 8-point n-butanol scale as a reference. n-butanol is used as a reference odour for trained panellists conducting sensory analysis. By using an 8-point n-butanol scale as a reference, the panellists can assess the odour intensity immediately (Q. Zhang et al. 2002). n-butanol is a primary alcohol with a characteristic mildly alcoholic odour (Biotechnology Information 2021). Each point on the scale correlates to an n-butanol concentration in the air, given in parts per million, representing a level of olfactory annoyance. Table 3.9 shows the n-butanol scale and the corresponding annoyance level.

Table 3.9: n-butanol 8-point scale with the corresponding annoyance level (Q. Zhang et al. 2002)

Level	n-butanol concentration in air [ppm]	Annoyance scale
1	12	Not annoying
2	24	A little annoying
3	48	A little annoying
4	960	Annoying
5	194	Annoying
6	388	Very annoying
7	775	Very annoying
8	1550	Extremely annoying

3.3.1   Odour Detection Threshold

In literature, the odour threshold is usually defined in one of two ways. The first method defines the threshold as the point when the odour is detectable from the neutral background odour. Another definition is when a trained observer can accurately identify the odorous composition of the odour sample (Leonardos, Kendall, and Barnard 1969). Regardless of the method used to define the threshold, the odour detection threshold (OT) is the point when 50% of the panel members perceive the odour. It is used to determine the odour concentration (Cod) in dynamic olfactometry by calculating the geometric mean of the OT measurements (Conti, Guarino, and Bacenetti 2020). Table 3.10 show the odour detection threshold for some common VOCs (Leonardos, Kendall, and Barnard 1969). It shows at what concentration, given in parts per million, the odour is detectable at.

Table 3.10: The odour detection threshold for some common VOCs, presented in ppm. Based on (Leonardos, Kendall, and Barnard 1969) and EPA

Chemical	Odour Threshold	Source
Acetaldehyde	0.21	Incomplete wood combustion, tobacco, motor vehicle exhaust, coal refining.
Benzene	4.68	Burning of oil and coal, motor vehicle exhaust, gasoline.
Formaldehyde	1.0	Building materials (especially from resins in particleboard products), cigarette smoke, combustion, paint, varnishes, laque, glue, cleaning products.
Methylene chloride	214.0	Paint stripper, propellant in aerosols, metal cleaning.
Tetrachloroethylene	4.68	Textile processing, metal cleaning.
Toluene	2.14	Paints, synthetic fragrances, ink, adhesives, cigarette smoke, motor vehicle exhaust, gasoline.
Xylenes	0.47	Paints, gasoline, motor vehicle exhaust, synthetic fragrances.

3.3.2 Percieved Air Quality

Perceived air quality (PAQ) is based on the human subject's perception of odour intensity (IO), air acceptability (AA) and percentage of dissatisfied (PD). This measurement system was first presented by Lars Gunnarsen and Per Ole Fanger (1992) and has been implemented in numerous PAQ studies since (Kraus and Senitkova 2019) (Senitkova and Kraus 2018) (Kolarik et al. 2014). The International Organization for Standardization (ISO) has also standardised the method in *ISO 16000-30:2014*.

Air Acceptability Scale

Air acceptability is evaluated on a scale from clearly acceptable (+1) to clearly unacceptable (-1), shown in figure 3.6. Both ISO 16000-30:2014 and Gunnarsen and Fanger operate with the same scale set-up. The panellists are presented the scale and are asked, "Imagine you are exposed to this odour in your everyday life. How would you rate this odour on the following scale?" (ISO 2014).
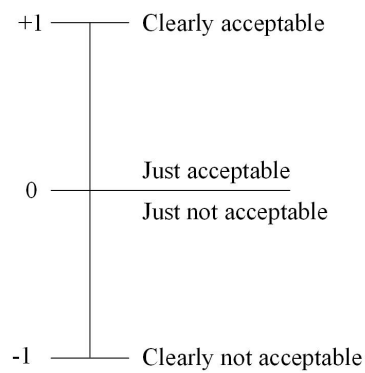
Figure 3.6: Air acceptability scale (AA), based on (Gunnarsen and Fanger 1992)

The percentage of dissatisfied also relates to how acceptable the air quality is. However, this time the acceptability is answered as a *yes* or *no* question and not rated along a scale. The panellist are asked; "Imagine you are exposed to this odour in your everyday life. Would you consider this odour acceptable?" (ISO 2014). The number of dissatisfied people i.e. the people who answered *No* is presented as n_d in equation 3.33, and n is the total number of people.

$$PD = \frac{n_d}{n} \times 100\%$$ (3.33)

Odour Intensity Scale

Gunnarsen and Fanger evaluate odour intensity on a five-point scale from no odour (0) to overwhelming odour (5), while the ISO standard uses a six category scale. The ISO scale is shown in figure 3.7. As this scale is designed to be used by untrained panel members it has a somewhat lower level of detail than the n-butanol 8-point scale shown in table 3.9.
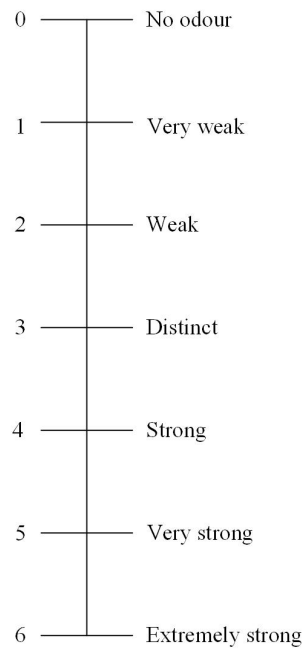
Figure 3.7: Odour intensity scale (OI), based on (Gunnarsen and Fanger 1992)

Hedonic Tone Scale

The hedonic tone of an odour describes how pleasant or unpleasant a person finds the smell. How pleasant the odour is perceived is often related to the odour intensity and air acceptability (Andrew Dravnieks, Masurat, and Lamm 1984). The hedonic tone scale is a nine point scale from the ISO standard for indoor air. It ranges from very pleasant (+4) to extremely unpleasant (-4), as shown in figure 3.8.
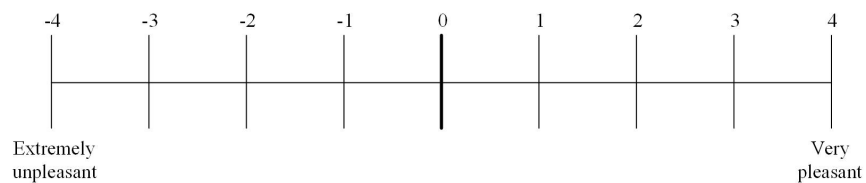
Figure 3.8: Hedonic tone scale for determining the pleasantness of the odour. Based on (ISO 2014)

Chapter 4

Description of the Test Rig

The MEE test rig was built in conjunction with Peng Liu's doctoral thesis at NTNU in 2016. Since then, it has been used in several project works and master's theses.

The test rig consists of the membrane energy exchanger core, contraction and expansion diffusers, pipes, air straighter, fans, measuring equipment and the supply and exhaust area (environmental chamber and laboratory). A description of the MEE core is provided in subchapter 4.3. Contraction and expansion diffusers are used to connect the rounded duct pipes to the rectangular inlets and outlets of the MEEs core. Two of the pipe sections have air straighteners installed to reduce turbulence before the airflow rate is measured. The supply air is drawn from the environmental chamber using two fans, one before the exchanger core and one after. The same setup is used for the exhaust air drawn from the laboratory. By controlling the fans, the pressure loss can be regulated by balancing the supply and exhaust air stream and minimising the air leakage. The environmental chamber is fitted with two CO_2 evaporators, which can provide air temperatures of between -35 to +20 $^\circ C$.
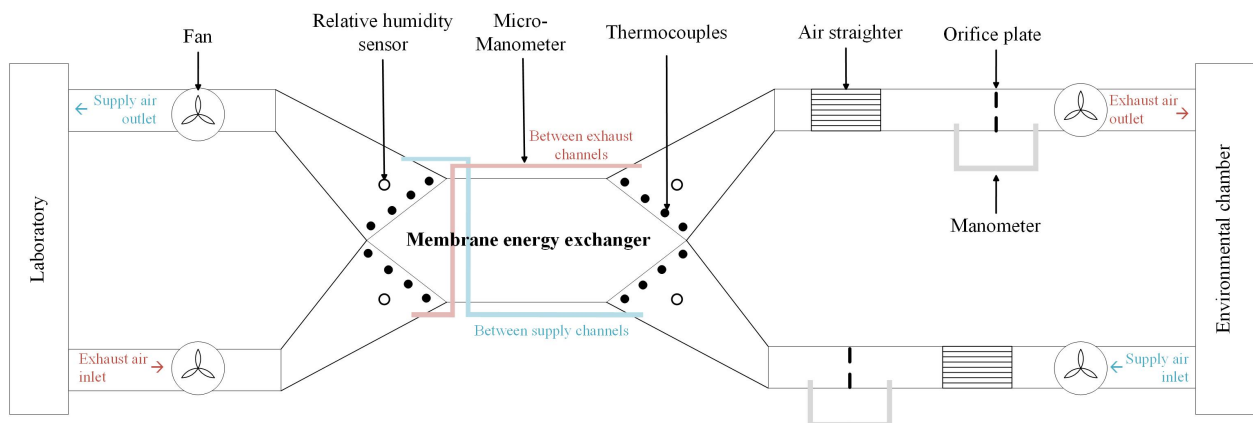
Figure 4.1: Schematic drawing of the MEE test rig, based on figure from (Liu et al. 2016)

Figure G.3 and G.4 shows pictures from the actual test rig. The numbering correlates to different parts of the MEE test rig, where: **1** - MEE core; **2** - Micro-manometers; **3** - Thermocouples; **4** - Relative humidity sensor; **5** - Environmental chamber; **6** - Severed ventilation channel connection; **7** - Odour inlet-hood; **8** - Computer with LabVIEW; **9** - Pipe leading to the basement exhaust; **10** - Air straightener; **11** -

Orifice plate with tubes leading to two manometers. More information about part **6**, **7** and **9** is provided in subchapter 4.2.
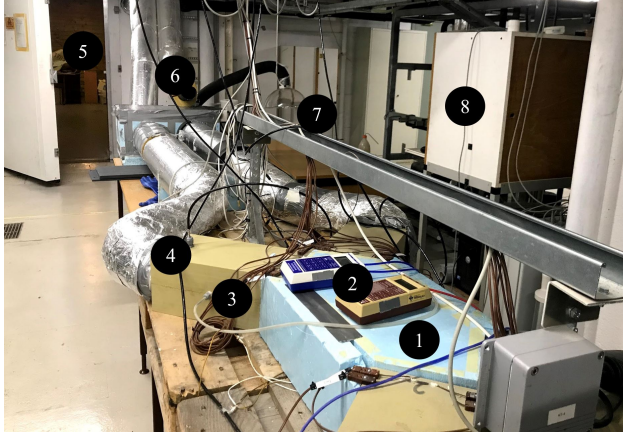
Figure 4.2: Picture of test rig from MEE core to environmental chamber.
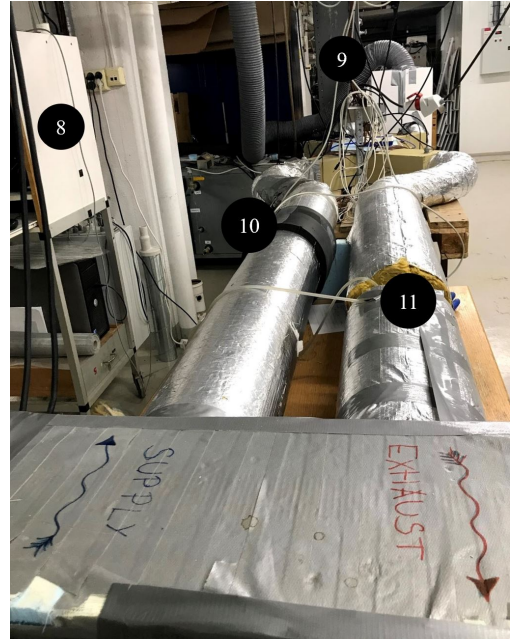
Figure 4.3: Picture of test rig from fans.

4.1 Placement of Sensors

There are several types of sensors connected to the test rig used to monitor the performance. Equipment measuring temperature and humidity in the MEE test rig is placed in each of the four diffusers. A temperature sensor is also placed in the environmental chamber. They are connected to a data-logging program called Labview which shows and logs the measurements automatically at a chosen time interval. Figure 4.4 shows a screenshot of the MEE test rig in LabVIEW. It gives an approximate placement of the temperature and humidity sensors. The temperature sensors are T-type thermocouples from the manufacturer Pettersen^{TM}. Humidity is measured using Vaisala^{TM} transmitters (HMT330) which log both humidity and temperature. Table 4.1 shows the operating conditions and accuracy of the measurement equipment installed at the MEE test rig.

Table 4.1: Measurement devices installed at the MEE test rig (Peng 2016).

Sensor	Operating conditions	Accuracy
Pettersen^{PM} T-type thermocouple	$-20°C$ to $+20°C$	$±0.05°C$
Vaisala^{PM} HMT330 humidity sensor	$-20°C$ to $+40°C$	$±0.8\%$ of reading $±1\%$ RH
KIMO$^®$ CP101 manometer	-500 Pa to $+1000$ Pa	$±1.5\%$ of reading $±3$ Pa
DPM^{PM} TT470S micromanometer	$0°C$ to $+50°C$	$±1\%$ of reading $±0.1$ Pa
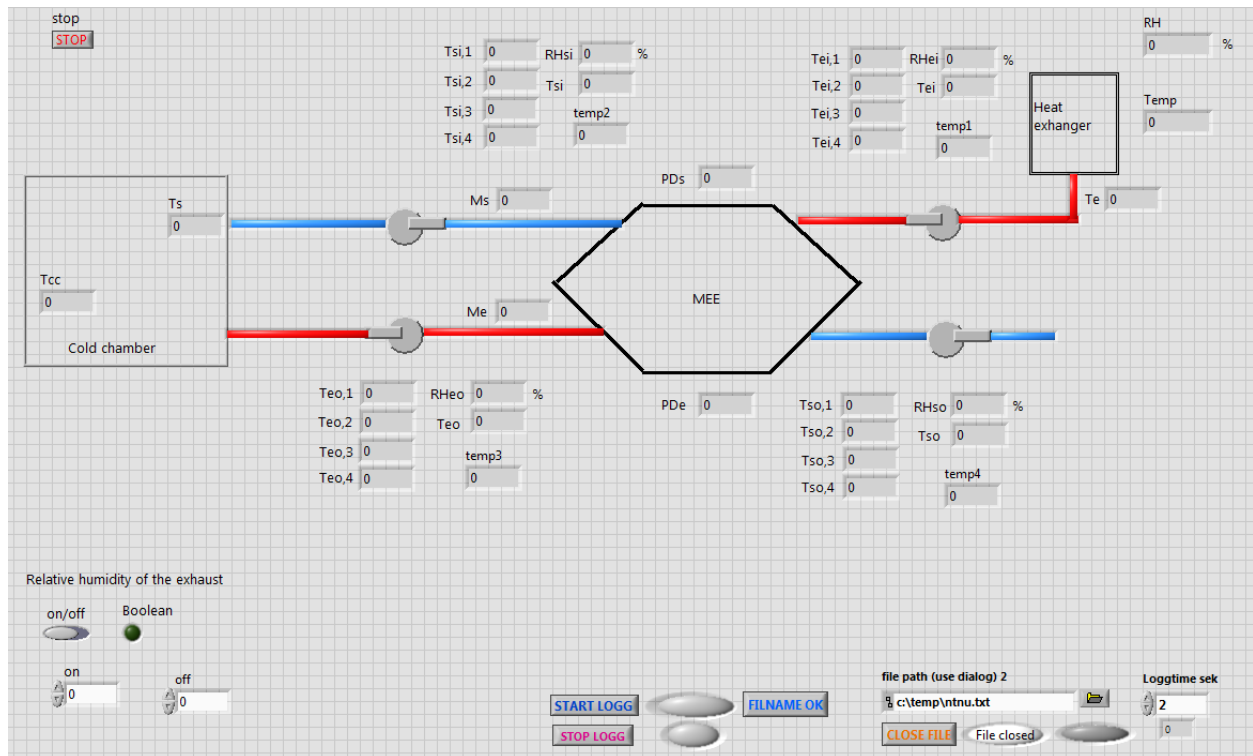
Figure 4.4: Screenshot of the test rig in LabVIEW.

The volumetric flow rate and pressure drop over the MEE has to be measured manually by reading the values from the equipment. The volumetric flow rate is measured using orifice plates. They are installed in the rounded pipes connected to the environmental chamber and measures the pressure drop across the plate with KIMO® manometers (CP101). Air straighteners are placed in front of the orifice plates because the orifice plate require a certain length of pipe section to get a valid result due to turbulence. The measured value is given in Pascal $[Pa]$ it needs to be converted into volumetric airflow rate $[L/s]$. This is done with an Excel sheet based on the standards NS-EN ISO 5167-1 and NS-EN ISO 5167-2. The pressure drop over the MEE core is measured with static pressure sensors connected to the inlet and outlet of the air stream. The pressure drop can be read directly from the connected micro-manometers from DPM^{TM} (TT470S).

4.2 Changes on the Test Rig

In order to conduct VOC and odour experiments on the test rig, some alterations had to be made. The new test rig configuration is shown in figure 4.1. The main adjustment was changing the definition of the direction for the supply and exhaust air. This is done to create an enclosed area in the environmental chamber to conduct the odour experiments. It is possible since the odour experiment does not require any conditioning of the supply air provided by the CO_2 evaporators in the chamber. The clean supply air is now drawn from the laboratory, and the exhaust air inlet comes from the ventilation hood where the odour is inserted. Because the odour source is supplied before the fan, this creates suction which draws the odour into the system. The exhaust air outlet from the test rig is connected to the basement ventilation system to help balance the system. It also ensures that the odour is not released into the surroundings and possibly interfering with the supply air from the laboratory.
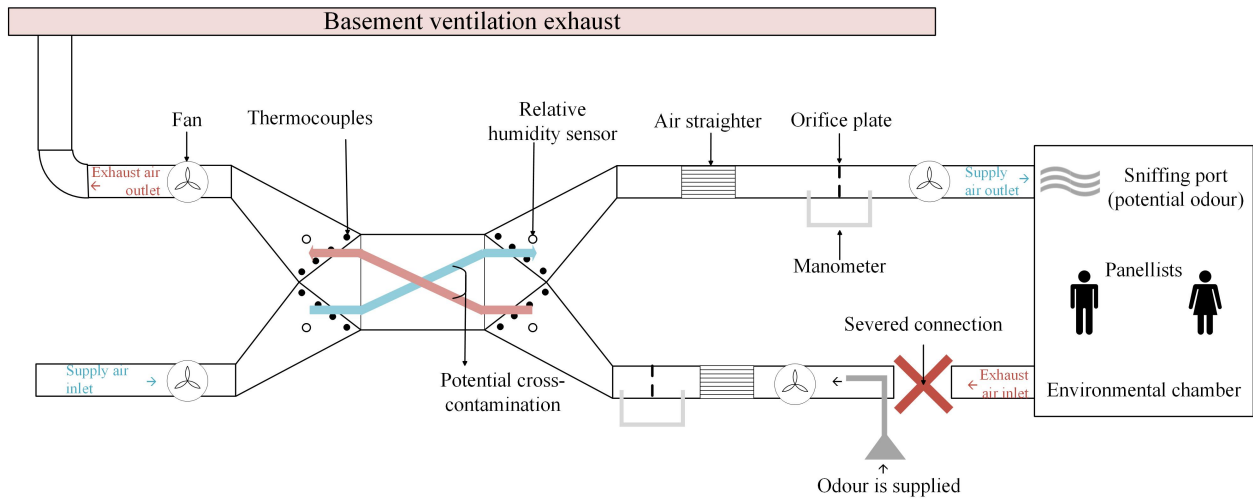
Figure 4.5: Schematic drawing of the MEE test rig, based on figure from (Liu et al. 2016)

The experiment's main objective is to investigate any cross-contamination between the odorous exhaust air and the clean supply air inside the membrane energy exchanger core. A tube is therefore connected to the supply air outlet to create a direct sniffing port. A sniffing port is used because the environmental chamber has a large volume of around 80 m^3. It would therefore take a considerable amount of time to disperse the odour evenly throughout the room. In addition, the sniffing port can reduce the interference of other odorous substances present in the room because the measurement is carried out quickly at the source. Figure 5.2 in subchapter 5.2 shows the sniffing port in question.

4.3   Exchanger Core Configuration

The membrane energy exchanger core has an elongated hexagonal shape due to its quasi-counter flow configuration. The inner and outer dimensions for the exchanger core are presented in table 4.2.

Table 4.2: Dimensions for the channels in the MEE core and headers

Parameter	Value	Unit
Number of membrane layers	9	-
Number of channels for each flow, n	18	-
Exchanger width	0.25	m
Exchanger length (counter-flow part)	0.4	m
Duct height, a	2×10^{-3}	m
Duct width, b	1.77×10^{-1}	m
Hydraulic diameter, D_h	3.96×10^{-3}	m

The MEE core is made out of the membrane, aluminium spacers and sealing brackets and a casing in plastic. Each sheet of the membrane is fitted with plastic brackets on both sides of the outer edge to create the air channels measuring 2 mm high. Nine sheets of the membrane material are used, creating 18 channels for the supply and exhaust air. The membrane is also sandwiched between sheets of corrugated aluminium

mesh to prevent the membrane layers from adhering to each other. Figure 4.6 shows how the membrane, spacer and brackets are fitted together. All layers are then enclosed with plastic plates on every side and glued together to create a tight seal.
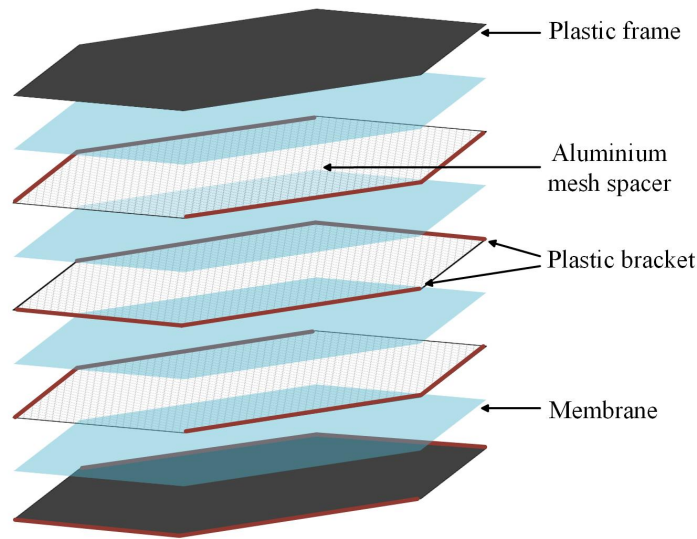
Figure 4.6: A simplified construction drawing of the MEE core showing the layers of membrane, spacer and brackets, based on a figure from Liu et al. (2016)

A detailed close up of the exchanger core is presented in figure 4.7. The figure shows that the corrugation of the aluminium mesh spacer creates a three-dimensional shape with a height of 2 mm. In order to achieve the corrugated shape, the mesh is placed in between two moulds and pressed into shape. The mould used to create the corrugation is shown in figure 4.8, and the resulting mesh spacer is shown in figure 4.9.
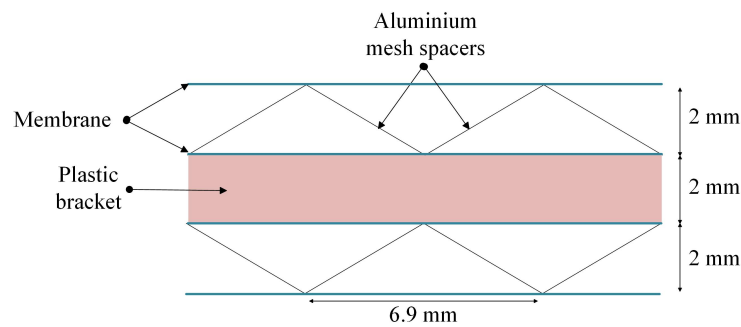
Figure 4.7: Membrane and spacer configuration in the MEE test rig, based on a figure from Liu et al. (2016)

Figure 4.8: The corrugated mould used to shape
the aluminium mesh spacers.
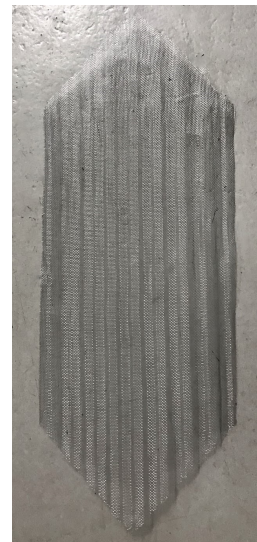
Figure 4.9: The mesh spacer after being shaped.

4.3.1 Membrane Materials

The membrane currently installed in the test rig core is made of polypropylene. This is a porous membrane with hydrophobic properties. Table 4.3 shows the physical parameters for the polypropylene membrane.

Table 4.3: Physical parameters for the polypropylene membrane

Parameter	Value	Unit
Thickness, δ	3.2×10^{-5}	m
Thermal conductivity, λ	0.16	$W/(mK)$
Diffusivity, D	2.42×10^{-5}	m^2/s
Permeability, P	1.6×10^{-12}	m^2/s
Density, , ρ	370	kg/m^3
Porosity, ϵ	41 %	-

The MEE core fitted with this membrane was built for Liu Peng's doctoral work in 2016 and has since been investigated in several other master's theses at NTNU. Due to the age and the many experiments conducted with this membrane, it is impossible to guarantee that it has maintained its physical properties. The membrane was tested for formaldehyde transfer in a master's thesis in 2019, and results indicated a large transfer through the membrane.

Flexit AS, the owner of the research project *Defreeze MEE Now*, has acquired two additional membranes called membrane No.16 and No.17. Both membranes are categorised as porous, with membrane No.16 being a plastic material and membrane No.17 being a paper material. Through some preliminary tests conducted at the SINTEF laboratory, the thickness and water vapour resistance has been determined. The results are displayed in table 4.4. There are some questions regarding the accuracy of the water vapour resistance measurements so further research should be conducted.

Table 4.4: Physical parameters of membrane No.16 and No.17

Parameter	No.16	No.17
Thickness, δ $[m]$	2×10^{-5}	1.2×10^{-4}
Water vapour resistance, μ $[m^2 s Pa/kg]$	0.133×10^8	0.156×10^8

5

Measurements

This chapter presents the method of the experiments that are preformed on the MEE test rig. Measurements on effectiveness and pressure drop where conducted during the preliminary study, and the method is therefore the same. The method for odour measurements is also based on the preliminary study as one of the tasks where to investigate possible odour measurement techniques.

5.1 Effectiveness and Pressure Drop Measurements

Latent and sensible effectiveness was measured during the preliminary study through experiments conducted at the MEE test rig. When the effectiveness measurements were carried out, the original test rig design (fig. 4.1) was used. During the experiment the supply air temperature was varied between -10°C and +10°C. To control the relative humidity the water spray nozzle is turned on in 30-second intervals, followed by a 20-second break. The relative humidity in the system is kept quite stable at 35% throughout the whole experiment.

After changing the temperature or volumetric flow of the system, the MEE needs some time to stabilise. When this is achieved, the logging function in Labview is turned on, measuring the temperatures and relative humidities of the thermocouples and transmitters every 76 seconds. The experimental sensible and latent effectiveness for the membrane energy exchanger could then be calculated with equation 5.1 and 5.2 (Liu et al. 2016).

$$\epsilon_S = \frac{t_{so} - t_{si}}{t_{ei} - t_{si}}$$
(5.1)

$$\epsilon_L = \frac{w_{so} - w_{si}}{w_{ei} - w_{si}}$$
(5.2)

Where the moisture content, w, is calculated with equation 5.3.

$$w = \frac{RH \cdot 10^7}{6.462 exp(\frac{5419}{T})}$$
(5.3)

The volumetric flow rate and pressure drop over the MEE is measured manually by reading the values from the measurement equipment. The pressure drop was measured also measured at five different supply air inlet temperatures, as well as four different volumetric airflow rates for each temperature.

5.2 Odour Measurements

Odour measurements are more comprehensive to conduct because they often depend on the sensory perception of humans. After all, the human nose is more sensitive to odours than instrumental detectors. There are standardised odour measurement techniques like dynamic olfactometry and field inspection. These methods require a continuously screened and trained group of panellists, making the odour measurement time consuming and expensive. A method that is more accessible and suited for a study of this magnitude is measurements of perceived air quality. The method was initially investigated in the preliminary study leading up this master's thesis. Subchapter 3.3.2 describes the PAQ method, and the corresponding odour measuring points; air acceptability, percentage of dissatisfied, odour intensity and hedonic tone. All the odour related questions were combined into one brochure which could be easily distributed during the experiment. The brochure is attached in appendix B.

5.2.1 Odour Samples and Dispersion Method

The choice of odour sample can significantly affect the experiment. Different odorous substances have different molecule size, which dictate if they can penetrate the membrane. The boiling point of the compounds will also influence the olfactory sensation as it describes the volatility. Higher volatility leads to more emitted particles from the samples, increasing the concentration in the air. In the odour experiment, five common household odour sources are used. They come from both natural and chemical sources and are listed below. Two *blank* samples are also tested, meaning no odour was used for these tests. The blank samples are included to assess the influence of the background odour and to validate the actual odour samples.

- Waffle
- Food waste
- Cleaning product
- Perfume
- Paint

The sample is placed below a ventilation hood to disperse the odour evenly into the air stream. A picture of the ventilation hood is shown in figure 5.1. The liquid samples, i.e. cleaning product and perfume, are sprayed onto a sponge placed underneath the hood. This method is chosen because using the spray nozzle would cause an uneven odour supply. The hood is connected to the exhaust air inlet channel. To the left in the picture (blue box) is a fan drawing in the odorous air. The original exhaust channel is severed to stop potential re-circulation of polluted air from the environmental chamber. By changing the airflow rate, the odour concentration can be controlled.

Figure 5.1: Ventilation hood connected to the exhaust air inlet.

Figure 5.2: Sniffing port connected to the supply air outlet.

Preliminary testing showed that it takes around 15 seconds from the odour is supplied until it is noticeable at the sniffing port, shown in figure 5.2. The time from when the odour sample is removed, until there are no more lingering odours, takes around 45 seconds. Based on this, the panel members are instructed to wait 30 seconds before they start sniffing after the odour sample is placed under the ventilation hood. When all panel members have evaluated the air, the sample is removed, and a timer is set for 1 minute before the experiment operator proceeds to the following sample. The samples are hidden from the panel members so that visual recognition is impossible. After smelling the odour, the members are asked to guess the odour source. The identification of an odour requires a more significant concentration than the recognition that an odour is present. This does not give a scientific result but can indicate how strong the odour is.

5.2.2 Selection and Instruction of Panel Members

The selection of panel members is based on the requirements established by the ISO standard for indoor air (ISO 16000-30:2014). The standard recommends that if an untrained panel carries out the perceived air quality measurements should consist of at least 15 persons, but ideally between 20 to 25 persons. If the panel consists of trained members, the number could be reduced to 8 persons (ISO 2014).

To be qualified as a panel member, the person should (ibid.):

- Be at least 18 years.
- Be motivated and available to complete the experiment.
- Have no health conditions or allergies which could affect the sense of smell.
- Avoid using personal hygiene products containing perfume.
- Ideally not smoke or use tobacco; however, they can participate if they refrain from tobacco two hours before and during the experiment.
- Not eat, chew gum or drink anything except water during the last 30 minutes before the experiments.

Panel members are usually kept in a well ventilated and low-stress environment in the last 30 minutes before the measurements are carried out. However, the location used in this experiment has no ventilation system. It is therefore impossible to provide a good air supply and remove background odours. The test rig in itself also has some built-in odour due to degassing from materials. Panel members are therefore introduced to the test environment a short period before the measurements start. This way, they can familiarise themselves with the odour and hopefully be able to distinguish between the background

odour and the new odour that is introduced. They are also given a short introduction to their tasks during the experiment. A brochure containing the scales for perceived air quality, air acceptability, odour intensity and hedonic tone is handed out. The brochure is shown in appendix B.

The panel members evaluate five different odour sources and two blank samples. The panel members are asked give their immediate evaluation of the air when they enter the test chamber. If a panel member cannot assess the air acceptability or odour intensity within 90 seconds, the assessment will be repeated after a 5-minute break. The panellists are prohibited from discussing their odour sensation with each other as this can influence their personal opinion.

5.3 VOC Measurements

In order to investigate the contaminant transfer through the membrane, a VOC sample is placed in the supply air stream. The concentration is then measured at each of the four inlets and outlets of the MEE core to investigate crossover. The VOC chosen for this experiment is formaldehyde, a common VOC in the indoor air, and one of few which can be readily measured (US EPA 2018). Formaldehyde is considered carcinogenic to humans and can not be used in a pure gas form due to regulations at NTNU. The solution is to use a particleboard assembled with a formaldehyde resin. When the particleboard is wetted, it should emit a measurable about of formaldehyde. The board is placed in the environmental chamber as this represents the indoor environment where most sources of formaldehyde are found.

Preliminary tests have shown that the air in the basement where the test rig is located already contains formaldehyde. This is because the basement acts as a storage space for the rest of the laboratory and probably holds materials containing a formaldehyde resin. Since the supply air in the system is drawn from the laboratory, this could impact the measurements. In order to determine the potential influence of the preexisting formaldehyde concentration, the particleboard is inserted into the environmental chamber 30 minutes after the measurements have started. This will record the increase in formaldehyde concentration coming directly from the board and make it easier to disregard the preexisting concentration in the basement air.

The sensor used in this project was developed and produced by Maria Justo Alonso for her doctoral research. The sensor consists of four sensor modules; SCD30 (CO_2, temperature and humidity), SPS30 (PM2.5 and PM10), SGP30 (TVOC) and WZ-S (formaldehyde). Table 5.1 shows the technical specifications for the formaldehyde sensor. All the sensors are placed on an Arduino board in an open plastic case measuring 24.5 cm $\times$ 15 cm $\times$ 6.5 cm. Figure 5.3 shows the sensor in question. The outputs are transmitted to a Raspberry Pi, where it is logged and stored as .csv-files. When the experiment starts, the sensors need about 20 minutes to stabilise. All measurements taken before this should therefore be disregarded when analysing the results.

Table 5.1: Technical specifications WZ-S sensor

Parameter	Value
Detectable Gas	HCHO
Detection Range	0-2 ppm
Overload	10 ppm
Resolution	0.001 ppm
Operating temperature range	$-20°C$ to $50°C$
Operating Humidity Range	10% to 90% RH (non-condensing)
Lifetime	5 years in air

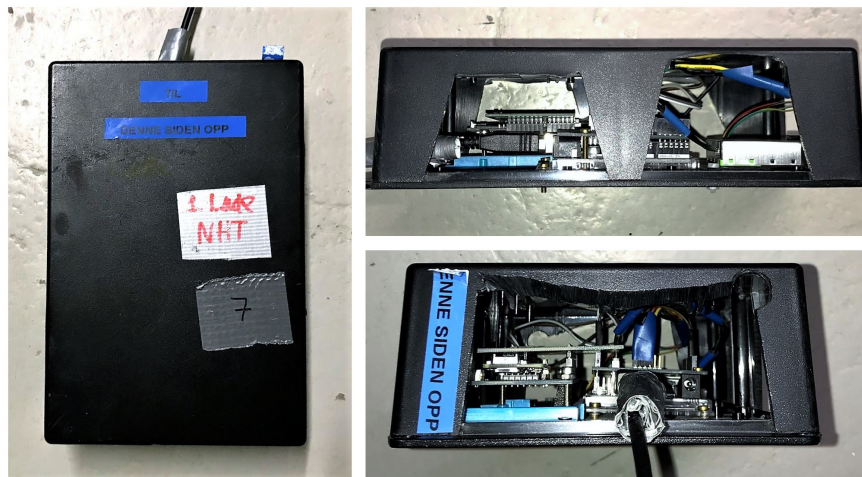Figure 5.3: The VOC sensor seen from different sides to show how the sensor modules are connected together.

Four sensors of this type are used to measure the formaldehyde transfer for the membrane energy exchanger at each of the supply and exhaust sides. Because sensors are larger than the pipes at the test rig, cardboard boxes or larger pipe sections were installed to fit them. Figure 5.4 shows how such a cardboard box is used.

Figure 5.4: Cardboard box installed at the exhaust air outlet in order to fit the VOC sensor.

The formaldehyde measurements are conducted at the original test rig design (fig. 4.1). However, the measurements are conducted at room temperature without conditioning the supply air from the environmental chamber. The measurements are repeated at three different airflow rates; 4.2 L/S, 6 L/s and 7.3 L/s.

5.4 Air Leakages

Air leakage measurements are carried out to investigate the air tightness of the system. Both the internal leakage between channels and the external leakage between the system and the ambient air is investigated. Tracer gas is inserted into the system to measure the potential leakages. An ideal tracer gas must fulfil specific requirements. It should not be hazardous towards humans or materials, i.e. non-toxic, non-flammable and non-allergenic. The gas should not react chemically or physically with other matters in the system. It must also be distinct from other gases so that a measuring equipment can measure it. The tracer gas chosen for this experiment is Nitrous oxide (N_2O), also known as laughing gas.

The legal limit for N_2O concentration is 50 ppm or 90 mg/m^3, set by the Norwegian Labour Inspection Authority (Ministry of Labour and Social Affairs 2011). The tracer gas is inserted into the system at a concentration of 25 parts/million fresh air. To achieve this, the volumetric airflow rate of the test rig must be known. With the help of a rotameter, the flow rate can be found. A rotameter is a simple and inexpensive instrument consisting of a tapered tube, usually made out of glass, with a metal float inside. The placement of the float indicates the speed of the gas leaving the container. In a natural state, the float is at the bottom of the tapered tube due to gravity, but it will be pushed up when the volumetric airflow rate increases due to drag forces. The accuracy of a rotameter is relatively low, at $\pm$ 2%. However, it still performs as well or even better than other high-tech flow meters (McAllister 2014).

Air leakage test using tracer gas are preformed at the maximum air flow rate of the system. Since

the volumetric airflow rate of the MEE test rig is relatively low, the concentration of N_2O in the system surpasses the legal limit. The rotameters can be controlled from 0 to 25 L/min, however, there are large increments between each value. In order to achieve a ppm of 25, the N_2O gas needs to be inserted at a rate of 0.02 L/min. Equation 5.4 shows how the tracer gas concentration is calculated, where Q_{tg} is the tracer gas flow rate in L/min and Q_v is the ventilation air flow rate of the system. To achieve this with the rotameters available at the lab, two rotameters need to be connected in series. The tracer gas is supplied before the fan in the severed pipe connection (see figure 4.5). The exhaust on the other side of the exchanger is connected to the basement ventilation. It is transported away from the system so that it will not interrupt the other measurements. There is a total of four measurement points, in each of the diffusers on every side of the exchanger. The measurement device is placed in the openings initially created for the micro-manometers.

$$\dot{Q}_{tg} = c_{tg} \cdot 10^{-6} \cdot Q_v \tag{5.4}$$

When the tracer gas is supplied, the concentration is analysed with one multi-point sampler and doser (Type 1303) and one multi-gas monitor (Type 1302) from Brüel & Kjær. Figure 5.5 shows a picture of the measurement equipment in question. The sampler and doser unit has six channels where it can measure the tracer gas concentration. Plastic tubes are connected to each channel and by suction the air sample is collected. Measurements are taken for one channel at a time and takes about one minute. There will therefore be a time-delay between measurements taken at different locations. The samples are analysed by the multi-gas monitor. With the help of the *Innova 7620 Application Software* from LumaSense Technologies the measurements are logged to a computer both numerically and graphically.
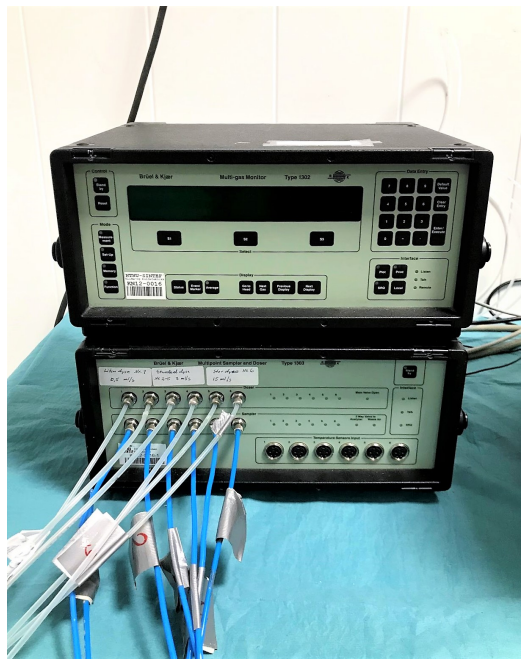

Figure 5.5: Brüel and Kjær equiptment for measuring the leakage in the exchanger with tracer gas. The monitor (Type 1302) is on top, and the sample and doser (Type 1303) is at the bottom.

5.5 Calibration of Equipment

Before measurements are carried out, the sensors should be calibrated to remove systematic errors and improve the accuracy of the measurements. The accuracy can change over time due to dust, shocks, wear and tear, and other contaminants. During calibration, the measuring equipment is compared to reference equipment. This equipment is traceable back to a national or international reference. Most measurement equipment should be calibrated at least once every year.

The individual sensors comprising the VOC sensor are already precalibrated by the manufacturers. However, additional verification of the accuracy can help to determine if there are any systematic errors. Subchapter 5.6 explains errors and uncertainties in more detail. Because the VOC sensor consists of several sensor modules, the calibration process requires several actions. The SCD30 sensor measuring CO_2, temperature and humidity is calibrated in two steps. The CO_2 accuracy can be calibrates using a reference CO_2 meter (Vaisala GM70 CO_2 Meter). Both meters are placed in a semi-enclosed box where a known amount of CO_2 is supplied. The temperature and humidity are calibrated with a reference instrument (Pegasor AQ^{TM} Indoor) placed in a small room without ventilation. A window is opened and closed to vary the temperature and humidity. The SPS30 sensor measuring particulate matter can be calibrated in the same room if some candles are burning during the experiments. The WZ-S formaldehyde sensor and SGP30 TVOC sensor cannot be calibrated because there are no appropriate reference instruments or methods. The pre-calibration from the manufacturer is therefore considered satisfactory (Gram 2019).

A simplified calibration can sometimes be conducted with the VOC sensors. It is done by placing the sensors outside in fresh air overnight to reset them.

5.6 Uncertainty Analysis

Errors and uncertainties are always present in a measurement. It is important to recognise them in order to minimise their impact on the result. Uncertainties in measurements are divided into three main groups (Novakovic et al. 2007).

- **Gross errors,** U_G - Due to lack of attention from the operator. Must be eliminated.
- **Systematic errors,** U_S - A constant error in the equipment or from the operator. Usually equal to the accuracy of the equipment and is given by the manufacturer.
- **Random errors,** U_R - Due to poor resolution in the equipment or other external influences. It cannot be eliminated but can be reduced.

5.6.1 Direct Measurements - One Variable

For equipment measuring only one variable, the result is given directly. Examples of direct measurements are temperature, relative humidity and gas concentration. However, there can be small variables between repeated measurements. To correct for the discrepancies, the mean value ($\overline{x}$, eq. 5.5) is calculated where $\sum x$ is the sum of the individual measurements, and n is the number of measurements. With the mean value, the standard deviation, s, can be found. Standard deviation is a measurement of the variation in the data set, calculated with equation 5.6.

$$\overline{x} = \frac{\sum x}{n} \tag{5.5}$$

$$s = \sqrt{\frac{\sum (x - \overline{x})^2}{n - 1}} \tag{5.6}$$

The random error, U_R, is calculated with equation 5.7. The systematic error, U_S, is given by the equipment manufacturer. The root sum square (RSS) value of these errors gives the resulting error, ΔU. This is shown in equation 5.8

$$U_R = \pm \frac{s}{\sqrt{n}} \tag{5.7}$$

$$\Delta U = \pm \sqrt{U_R^2 + U_S^2} \tag{5.8}$$

5.6.2 Indirect Measurements - Multiple Variables

Indirect measurements consist of multiple variables measured individually and then inserted into a formula to calculate the final output. Examples of such measurements are sensible and latent effectiveness and moisture content in the air. For these cases, the resulting error is calculated with equation 5.9. The equation assumes that the errors are independent of each other and is derived using the Taylor series.

$$\Delta U = \pm \sqrt{\left(\frac{\partial f}{\partial u_1} \cdot \Delta u_1 \right)^2 + ... + \left(\frac{\partial f}{\partial u_n} \cdot \Delta u_n \right)^2} \tag{5.9}$$

5.6.3 Accuracy of Sensory Assessments

The ISO standard for indoor air (ISO 16000-30:2014) defines the accuracy requirements for the odour experiments conducted at the test rig. A confidence interval determines the accuracy of these measurements. If the half-width of the 90% confidence interval of the mean does not exceed 0.2, the air acceptability assessment is considered accurate. For odour intensity and hedonic tone, the 90% confidence interval of the mean must not exceed 1 (ISO 2014). Equation 5.10 calculated the two-sided confidence interval for the odour measurements. In this equation, μ is the actual mean value, while $\overline{x}$ is the estimated mean value. α is the probability of error in the experiment.

$$P\left(\mu \, \epsilon \left[\overline{x} \pm \frac{s}{\sqrt{n}} \cdot t_{(1-\alpha/2);n-1} \right] \right) = (1 - \alpha) \tag{5.10}$$

where

$t_{(1-\alpha/2);n-1}$ is the $(1 - \alpha/2)$-percentile of the t-distribution.

Figure 5.6 shows a t-distribution plot. Related to the accuracy requirements for the sensory assessments, the statistical certainty, $(1 - \alpha)$, is 90%, and the probability of error, α, is 10%. The half-width of the 90% confidence interval is therefore 5%.
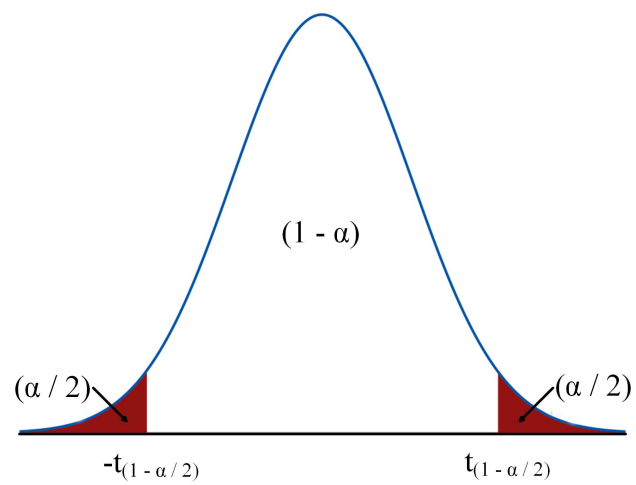
Figure 5.6: Two-sided t-distribution plot for the 90% confidence interval.

Chapter 6

Results

6.1 Effectiveness and Pressure Drop

Measurements on effectiveness and pressure drop were conducted on the MEE test rig during the preliminary study leading up to this master's thesis. The results are presented in this subchapter, as these findings are helpful when evaluating the total performance of the membrane. However, new graphs have been made to improve the presentation of the results.

6.1.1 Sensible and Latent Effectiveness

Figure 6.1 shows the sensible and latent effectiveness at different supply air temperatures. In the experiment, the volumetric airflow rate is set to the highest level on the test rig, which is 7.3 L/s. The graph shows that the sensible effectiveness is more or less the same for every supply air temperature, at $\pm$ 90%. The highest sensible effectiveness is reached when the supply air is set to $+5°C$. The sensible effectiveness decreases slightly as the temperature decreases. However, the supply air temperature at $+10°C$ does not follow this trend.

The latent effectiveness has some fluctuations throughout the experiment compared to the sensible effectiveness. However, it shows the same correlation between temperature and effectiveness as the sensible effectiveness does; low supply air temperature results in lower effectiveness. This trend stops at a specific temperature because the supply air temperature above $+5°C$ does not result in higher effectiveness. The average latent effectiveness for all the supply air temperatures tested is 70%.
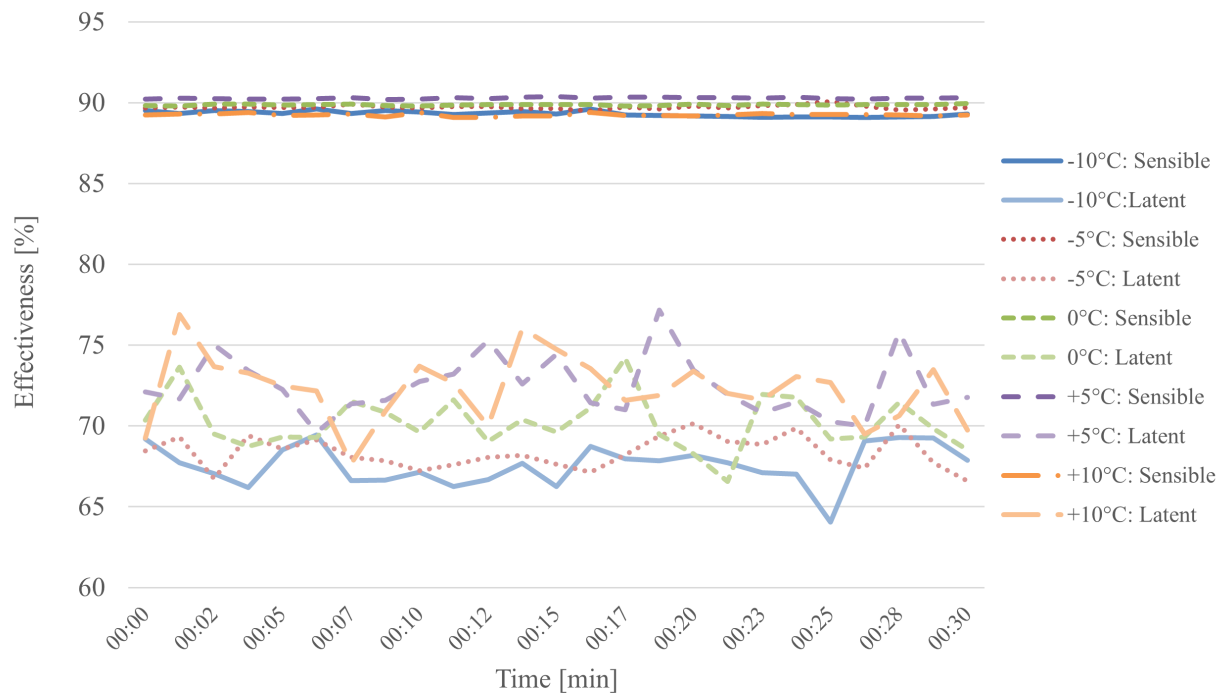
Figure 6.1: Measured latent and sensible effectiveness at different supply air temperatures

6.1.2 Pressure Drop

The new graph displaying the correlation between pressure drop and volumetric airflow rate is shown in figure 6.2. It includes additional data for when the supply air temperature is varied between -10$°C$ and +10$°C$. The graph also shows the pressure drop measured on both the supply and the exhaust side of the exchanger. Even though the measurements are conducted when the system is in balance, the two micro-manometers show different pressure drop values. It is worth mentioning that the manometer used on the exhaust side has the most recent calibration and is therefore assumed to be the most accurate. The volumetric airflow rate is varied between 2.7 and 7.7 L/s throughout the experiment. A linear trendline is added to the data points showing a correlation between the volumetric airflow and the pressure drop. When the airflow rate increases, the pressure drop increases. At the maximum volumetric airflow rate achieved at the test rig, the pressure drop is around 600 Pa, measured on the exhaust side.
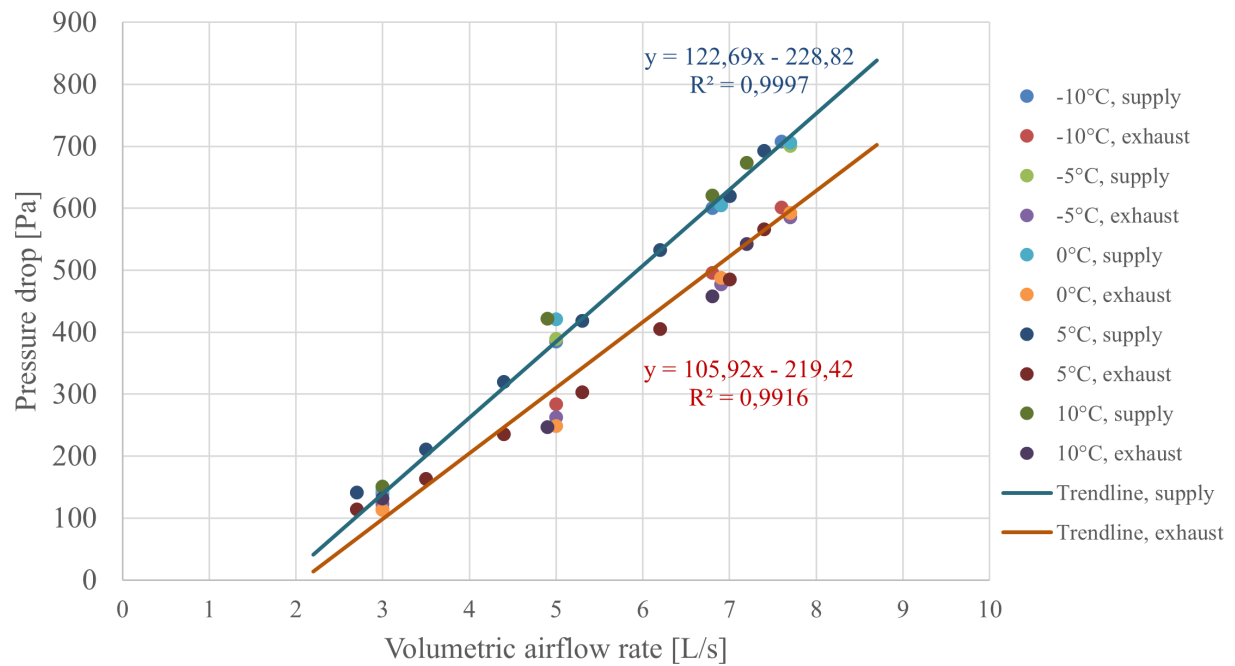
Figure 6.2: Pressure drop in the MEE core at different volumetric airflow rates.

The trendline for the pressure drop measured on the exhaust side has the function $y = 105.92x - 219.42$, with an R-squared value of 0.9916. R-squared values are calculated by squaring the correlation coefficient, and it describes how good the trendline fits the data points. An R^2 value of 1 has the best fit. The trendline for the pressure drop is therefore considered a good fit.

6.2   Odour Transfer

The odour experiment is conducted with a volumetric air flow rate of 7.3 L/s. The experiment is repeated seven times, with five different odour samples and two blank rounds with no odour. Table 6.1 shows the order that the odour samples are tested. The right section of the table shows what the panel members guessed was the odour source. Only sample number 4, 6 and 7 are guessed correctly by one or more panel members. However, the majority of panellists are unable to recognise the odour source.

Table 6.1: Order of odour samples during sensory experiment

Sample Number	Odour	Guesses
1	Paint	Perfume, soap
2	No odour	Perfume, soap, licorice, cleaning product, sweet
3	Cleaning spray	"Snus", sweet, food waste (milk), egg
4	Waffle	Waffle, potato, cake, egg,
5	No odour	Tobacco, coffee, nail polish remover, sweet
6	Perfume	Apple, perfume, paint, cleaning product, soap, oil
7	Food waste	Tobacco, food waste, sweet

6.2.1 Percentage of Dissatisfied

The panel members are first asked to answer *yes* or *no* on whether they considered the odour acceptable. Based on the answers, the percentage of dissatisfaction is calculated, shown in figure 6.3.
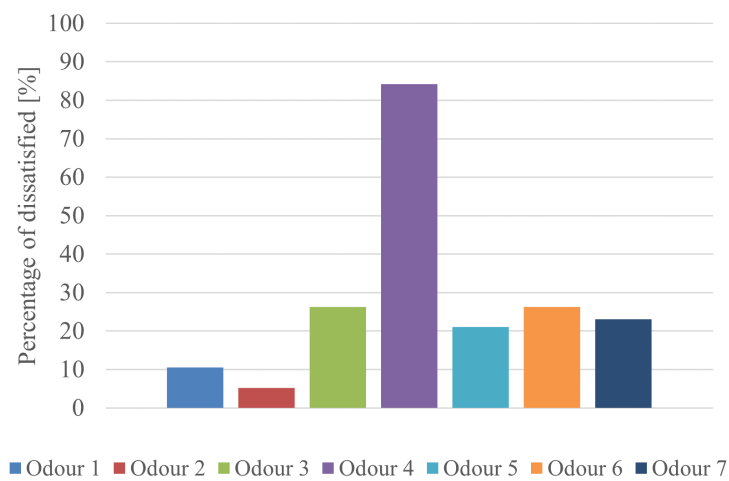
Figure 6.3: The calculated percentage of dissatisfied for each odour sample.

The two first odour samples receive similar feedback from the panel members, although the second sample is blank. Odour sample number 3, 5, 6 and 7 have similar percentages of dissatisfaction between 21.1 and 26.3%. It is worth mentioning that sample number 5 is also blank. The waffle odour is by far the odour with the highest PD with 84.2%.

6.2.2 Air Acceptability

Air acceptability is rated next by the panel members. This test is similar to the percentage of dissatisfaction. The only difference is that the panellists have the opportunity to rate the odour along a scale. The scale goes from *clearly acceptable* (+1) to *clearly not acceptable* (-1). Figure 6.4 illustrates the answers from experiment. Each of the coloured circles represents the evaluation from one panel member. The results are presented in this manner to display the large scattering of answers. This is because some panellists rated the air vastly different than the others. Table 6.2 shows the average air acceptability of each odour.
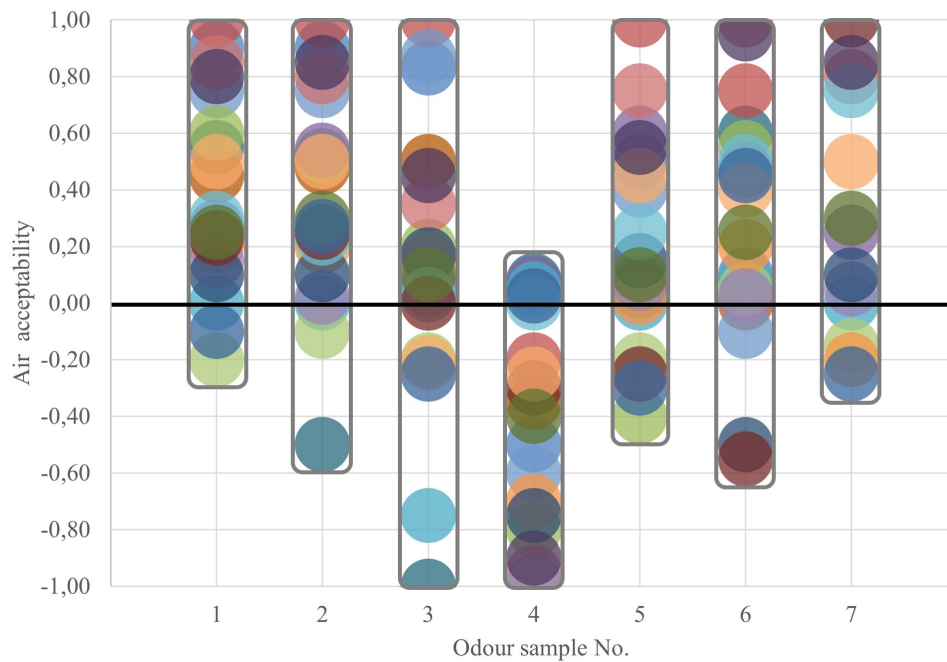
Figure 6.4: Air acceptability for each odour sample, were every panellists review of the odour is visualised with a coloured circle.

The first odour sample of paint has the highest average air acceptability at 0.40 and the least scattering. The second sample, which is blank, has somewhat lower air acceptability. This is because the interval of answers is larger than for the first sample, even though most panel members rated the air acceptability between 0 and 0.60. Odour sample 3 has the most extensive scattering of answers, ranging over the whole scale. The waffle odour has the lowest average air acceptability at -0.45. Most panellists rated the odour between 0 and -1, meaning they experienced it as *not acceptable*. Odour sample 5, which is blank, is rated as having lower air acceptability than the first blank sample. The average air acceptability for sample 5 is 0.20, compared to 0.37 for sample 2. However, the scattering of answers is quite similar. The perfume and food waste odour samples are rated quite similar in average air acceptability, at 0.28 and 0.31, respectively.

Table 6.2: The average air acceptability.

	No. 1 Paint	No. 2 No odour	No. 3 Cleaning product	No. 4 Waffle	No. 5 No odour	No. 6 Perfume	No. 7 Food waste
Average AA	0.40	0.37	0.12	-0.45	0.20	0.28	0.31

Odour sample number 2 and 5 are rated to have a higher average air acceptability than the other samples by 64% and 78% of panel members, respectively. These two samples are blank and used for comparison with the household odour samples.

6.2.3 Odour Intensity

Results from the odour intensity test is shown in figure 6.5. The intensity is rated from *no odour* (0) to *extremely strong* (6). Table 6.3 shows the average odour intensity for each sample.
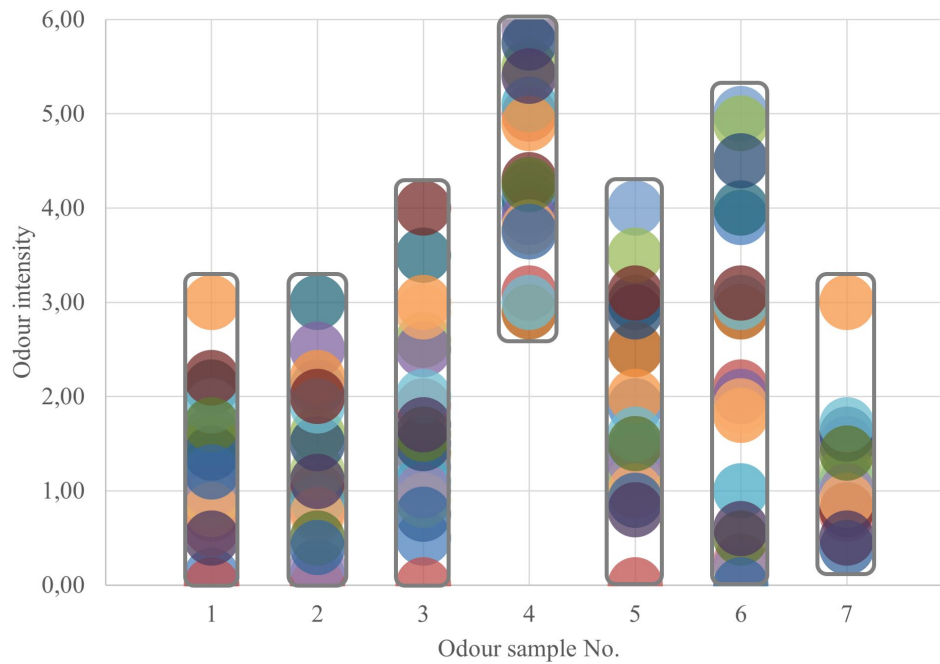
Figure 6.5: The odour intensity of each odour sample.

The two first samples have an almost identical average odour intensity at 1.24 and 1.25, respectably. However, the scattering of answers is a bit more compact for the paint sample. The cleaning product sample has an average OI of 1.86 and a relatively even scattering. Sample number 4, consisting of waffles, has by far the highest odour intensity. All panel members rated it between 3 and 6, with the average coming in at 4.45. Sample number 5 is blank but still has an average OI of 1.97. This gives a good indication of how strong the background odour in the test rig is perceived. The perfume odour sample has the second-highest OI, averaging at 2.42. However, the perfume also has the largest scattering of answers. Most panel members agree that the food waste odour sample has a low odour intensity and rate the OI between 0 and 2. The average value is 1.22, the lowest out of all odour samples. It is even lower than the blank samples.

Table 6.3: The average odour intensity.

	No. 1	No. 2	No. 3	No. 4	No. 5	No. 6	No. 7
	Paint	No odour	Cleaning product	Waffle	No odour	Perfume	Food waste
Average OI	1.24	1.25	1.86	4.45	1.97	2.42	1.22

The first blank sample is perceived to be less intense compared to the household odour samples by 63% of the panels members. Results from the second blank sample show that 50% of the panel members rate the odour as less intense.

6.2.4 Hedonic Tone

In the hedonic tone test, the panel members are asked to rate how pleasant or unpleasant they experience the odour. The results are given in figure 6.6.
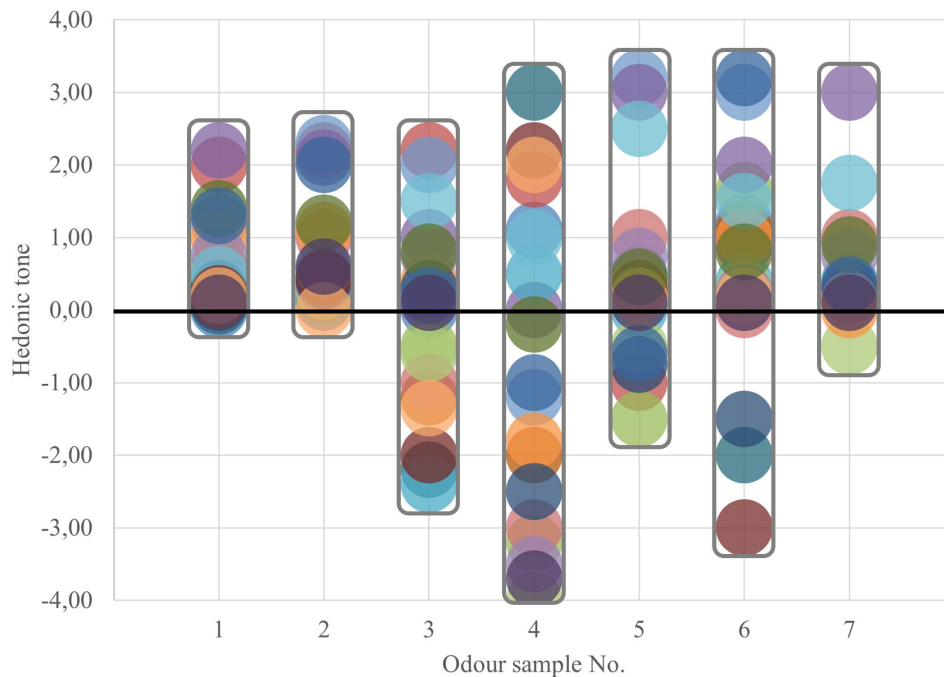
Figure 6.6: The pleasantness of each odour measured by their hedonic tone.

Similar to the previous odour tests, the hedonic tone of sample 1 and 2 are almost identical. Sample 2, which is blank, has the highest average hedonic tone at 0.64, compared to 0.52 for the paint. The third odour sample has a pretty uniform distribution of answers, ranging from -2.5 and +2.5. The distribution evens out the average hedonic tone score, which is at -0.10. The same uniform tendencies are seen in the waffle odour sample. Panel members have very different opinions on the hedonic tone, however, the majority rates it as unpleasant. The average HT is -0.75 for the waffle sample. The next odour the panellist evaluated is the second blank sample. It has a lot of scattering in answers, but most panellists rate the odour somewhere around zero. The average HT is lower for sample number 5 compared to sample number 2, at 0.34 and 0.64, respectively. The odour sample of food waste have some panel members rating is as quite pleasant, but the average lays at 0.53.

Table 6.4: The average hedonic tone.

	No. 1 Paint	No. 2 No odour	No. 3 Cleaning product	No. 4 Waffle	No. 5 No odour	No. 6 Perfume	No. 7 Food waste
Average HT	0.52	0.64	-0.10	-0.75	0.34	0.49	0.53

The majority of the panellists rate the hedonic tone of the odour samples as less pleasant than the blank samples. 64% for the first blank sample, and 69% for the second blank sample.

6.2.5 Uncertainty of the Sensory Assessments

Table 6.5 shows the mean values for air acceptability, odour intensity and hedonic tone, including the 90% confidence interval of the mean. Appendix **??** shows how the interval is calculated. The confidence interval must not exceed 0.2 for air acceptability and 1 for odour intensity and hedonic tone for the measurements to be considered accurate. The air acceptability for odour 3, the cleaning product, is exactly 0.2. However, all other values stay below the accuracy requirement.

Table 6.5: The mean values for the odour experiment and their 90% confidence interval.

	AA [-]	OI [-]	HT [-]
Odour 1	0.38 ± 0.14	1.21 ± 0.29	0.52 ± 0.09
Odour 2	0.37 ± 0.15	1.25 ± 0.34	0.64 ± 0.11
Odour 3	0.11 ± 0.20	1.87 ± 0.42	-0.10 ± 0.16
Odour 4	-0.45 ± 0.15	4.44 ± 0.39	-0.75 ± 0.29
Odour 5	0.18 ± 0.15	1.91 ± 0.42	0.34 ± 0.17
Odour 6	0.27 ± 0.17	2.41 ± 0.70	0.49 ± 0.20
Odour 7	0.30 ± 0.17	1.23 ± 0.24	0.53 ± 0.12

6.3 Formaldehyde Transfer

Figure 6.7 shows the preliminary measurements conducted to establish the background concentration of formaldehyde in the laboratory and environmental chamber. Based on the layout in figure 4.1, it is apparent that the formaldehyde concentration is highest in the exhaust inlet air coming from the environmental chamber. Here the concentration is $\pm$ 110 $\mu g/m^3$. Some more preliminary measurements are conducted and are shown in appendix D.

The formaldehyde concentration decreases considerably from the supply inlet to the supply outlet. It is lower than the concentration in the exhaust outlet air. This indicates that there is internal leakage in the exchanger core.
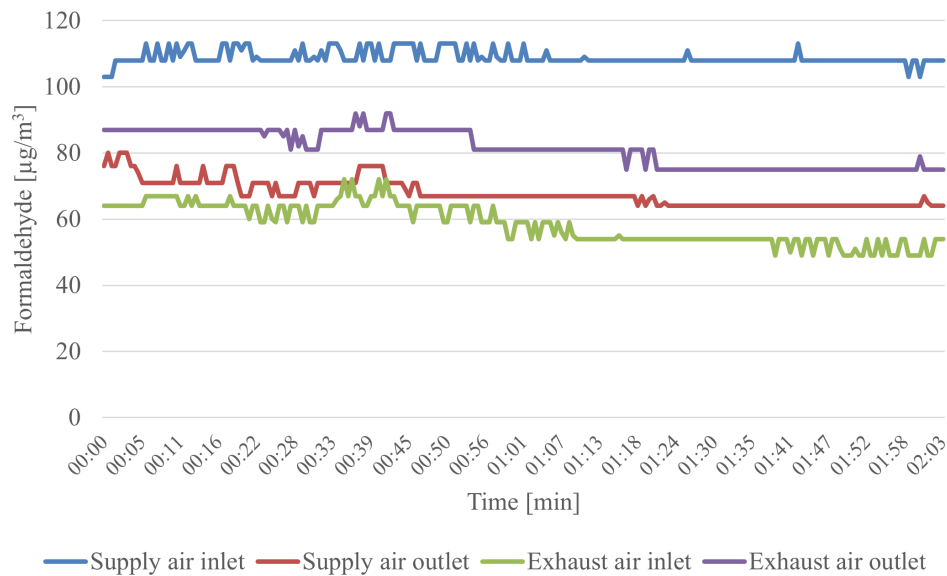
Figure 6.7: Preliminary formaldehyde measurements to establish the formaldehyde concentration in the basement and environmental chamber. Conducted at a volumetric airflow of 6 L/s.

Figure 6.8, 6.9 and 6.10 illustrates the formaldehyde concentration at the different inlets and outlet during the experiment. The experiment is repeated three times at different volumetric airflow rates; 4.2 L/s, 6 L/s and 7.3 L/s. The wetted particleboard containing a formaldehyde resin is inserted at the supply inlet channel 30 minutes after the measurements started. An increase in the formaldehyde concentration can therefore be seen on the graphs at this time.
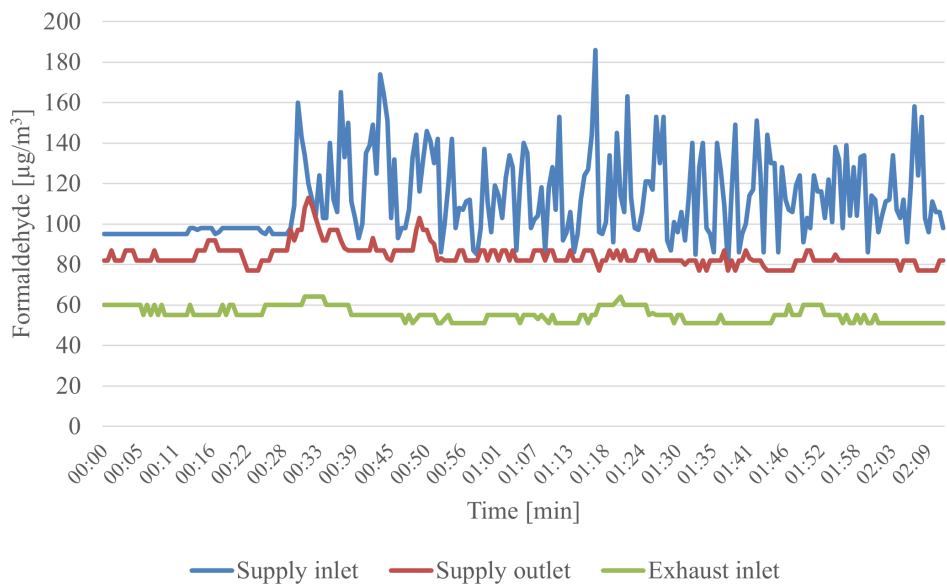
Figure 6.8: Measurement of formaldehyde transfer through the membrane at a volumetric airflow of 7.3 L/s.
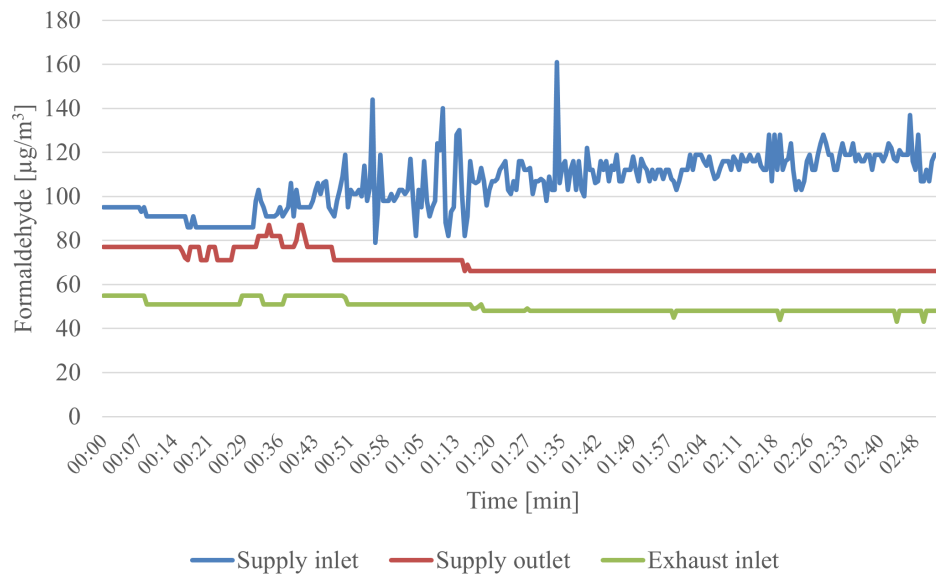
Figure 6.9: Measurement of formaldehyde transfer through the membrane at a volumetric airflow of 6 L/s.
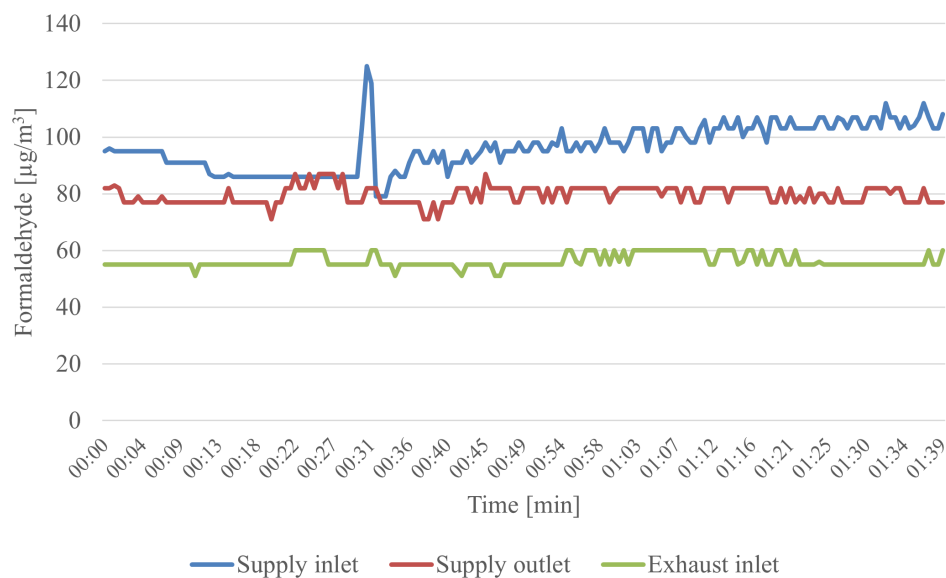
Figure 6.10: Measurement of formaldehyde transfer through the membrane at a volumetric airflow of 4.2 L/s.

The graphs show that the initial formaldehyde concentration in the supply inlet is just below 100 $\mu g/m^3$ during all three experiments. After the formaldehyde source is supplied, the concentration increases but fluctuates quite a bit. This is especially true for the higher volumetric airflow rates. It is also apparent that the formaldehyde concentration is higher when the airflow rate is high. The average formaldehyde concentration after the particleboard is supplied is 116.5 $\mu g/m^3$ at 7.3 L/s, 109.5 $\mu g/m^3$ at 6 L/s and 99.6 $\mu g/m^3$ at 4.2 L/s. However, the peak concentration of formaldehyde is measured to be even higher due to the large fluctuations. The formaldehyde concentration in the supply outlet and exhaust inlet experience a small increase after the particleboard is inserted, but is relatively constant throughout the experiment.

Table 6.6 shows the average exhaust air transfer ratio (EATR) for the three experiments. The EATR

is calculated both before and after the formaldehyde source is placed in the test rig. The rightmost column shows how much the ratio increases. It is calculated because the formaldehyde concentration is slightly different at the start of each measurement. Results show that the EATR increases when the volumetric airflow rate decreases, even when there is less formaldehyde in the system at the lower airflow rates.

Table 6.6: The exhaust air transfer ratio of formaldehyde for the different volumetric airflow rates.

Volumetric airflow rate [L/s]	EATR before [%]	EATR after [%]	Increase [%]
7.3	30.49	46.47	15.98
6	27.59	44.67	17.08
4.2	37.81	65.72	27.91

The crossover of formaldehyde has to be calculated using the preliminary measurements due to some problems with the equipment. The measurements used are shown in appendix D. Figure 6.11 shows the crossover calculated for the different volumetric airflow rates, calculated with equation 3.28. Similar to the EATR results, the crossover increases as the volumetric airflow rate decreases. The average crossover is 62.9% at 7.3 L/s, 74.8% at 6 L/s and 81.3% at 4.2 L/s.
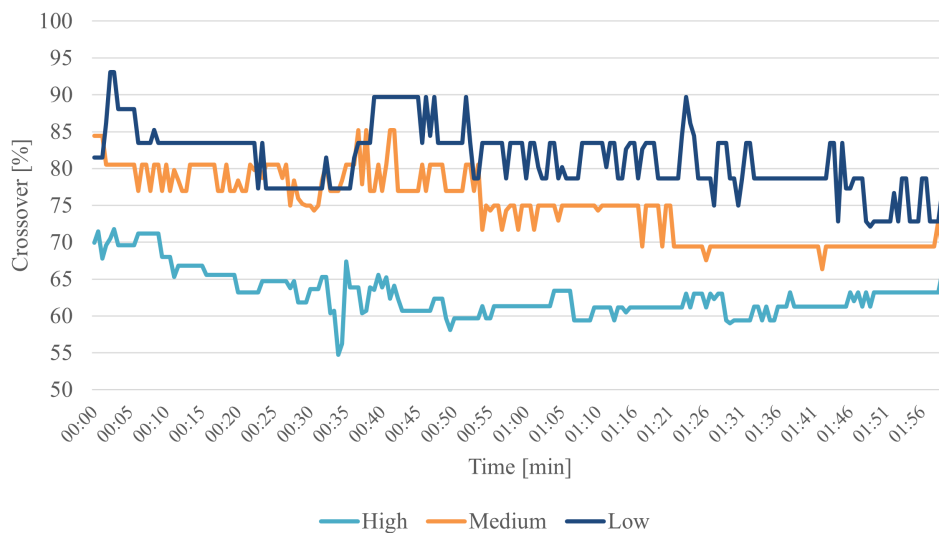
Figure 6.11: The calculated formaldehyde crossover for three different volumetric airflow rates.

6.4 Air Leakage

Figure 6.12 shows the measured air leakage through the MEE core. The experiment is conducted with a volumetric airflow rate of 7.3 L/s, and with a supply of 25 PPM of N_2O in the exhaust air inlet. The results show a decrease in the tracer gas concentration from the inlet side to the outlet side of 5.24%. This indicates a leakage, either internal and/or external. Due to a time delay of one minute between the measurements, the concentration is sometimes higher on the exhaust outlet than the exhaust inlet.

The change in tracer gas concentration is measured to be 1.67% from the supply outlet to the supply inlet. This indicates a small internal leakage. The concentration at the supply inlet side should ideally be zero, but due to the placement of the tracer gas sensors a small concentration can be measured.
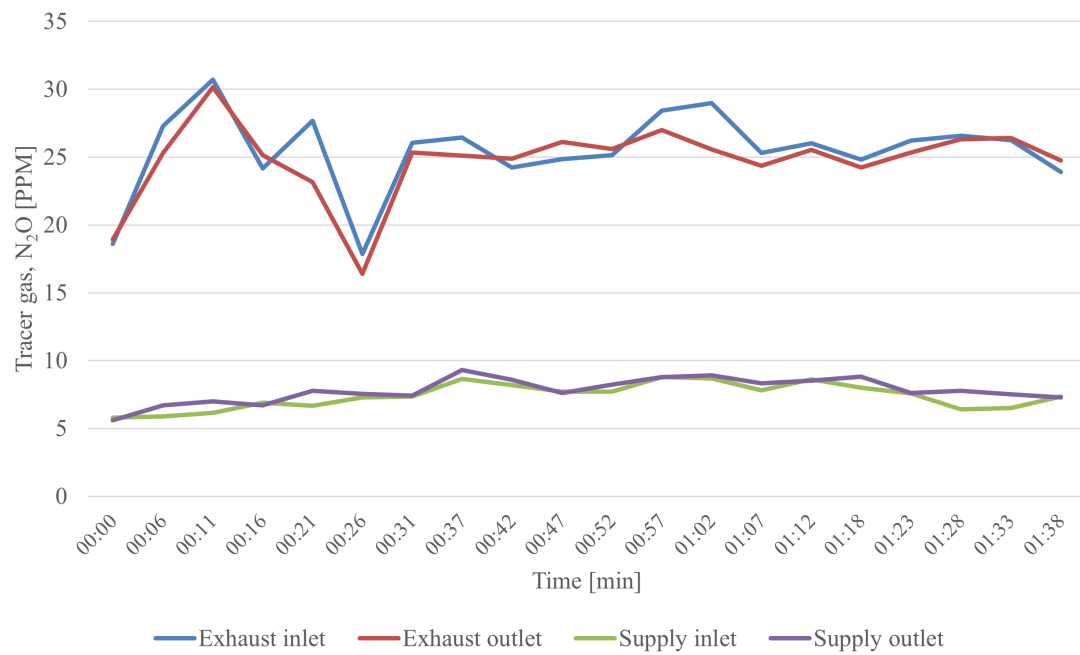
Figure 6.12: Measured air leakage with the help of the tracer gas N_2O

Table 6.7 shows the calculated recirculation fraction and change in tracer gas concentration. The supply and exhaust side recirculation fractions substantiates the findings. Based on the measured change in tracer gas, the external leakage is calculated to be 3.57%. This is supported by the exhaust side recirculation fraction, which is found to be 3.60%. The supply side recirculation fraction indicate a slightly larger internal leakage than initially measured, at 2.06%.

Table 6.7: Calculated recirculation fraction and change in tracer gas concentration

	Recirculation Fraction	Change in tracer gas concentration
Supply side	2.06%	1.67%
Exhaust side	3.60%	-5.24%

Discussion

This chapter aims to evaluate and discuss the findings from the experiments conducted at the test rig. The results from the different experiments will be compared and seen in a larger context to investigate the total performance of the membrane. In the last subchapter, the research questions will be discussed based on results and relevant literature.

7.1 Effectiveness and Pressure Drop Measurements

The effectiveness and pressure drop of the polypropylene membrane is measured during the preliminary study. In the preliminary study, the results only displayed the measurements at one supply air temperature. Therefore, new and improved graphs have been made showing the effectiveness and pressure drop for supply air temperatures varying between -10 and $+10°C$. This proved to be beneficial because it shows a connection between supply air temperature and effectiveness. With the exception of the measurements done at $+10°C$, the results show a decrease in both sensible and latent effectiveness as the temperature decreases. This tendency is not seen at $+10°C$ because the supply air is relatively close to the room temperature, and the MEE is therefore not working at maximum effect.

During the experiment, the sensible effectiveness stays relatively constant at 90% for all supply air temperatures. It is well established in the literature on energy exchangers that sensible effectiveness is not affected by temperature and humidity changes. However, latent effectiveness is affected by these thermodynamic changes to the supply air. This can be seen quite clearly in figure 6.1. The latent effectiveness varies $\pm$ 5 - 10% from the average through the experiment for all supply air temperatures. This is because the supply air temperature has some variations over time. Humidity also varies through the experiment because the spray nozzle supplying moisture is turned on and off in 30-second intervals, followed by a 20-second break. These variations make it clear that the latent effectiveness is affected by changes to the ambient air.

Pressure drop measurements were repeated at four volumetric airflow rates for each supply air temperature. Since pressure drop is not related to temperature, all measurements can be placed in one graph with a corresponding trendline. This trendline shows the pressure drop as a function of the volumetric airflow rate. The pressure drop of the MEE core is measured with two micro-manometers on both the supply and exhaust side, resulting in two trendlines. As shown in figure 6.2, the pressure drop is measured to be higher on the supply side compared to the exhaust side. Ideally, they should show the same result.

Since the fans in the test rig are balanced, the main reason for this difference is a systematic error in the measurement equipment. The accuracy of the DPM^{PM} TT470S micro-manometers is $\pm$ 1% of readings $\pm$ 0.1 Pa. However, as time goes by and the equipment is exposed to dust, shocks, wear and tear, the accuracy can be reduced further. The two micro-manometers have been calibrated at different times, which can explain the differences in results. The manometer used on the exhaust side has had the most recent calibration and is assumed to be the most accurate. This is why the results from just the exhaust side manometer is used.

The trendline for the pressure drop measured on the exhaust side has the function $y = 105.92x - 219.42$, with an R-squared value of 0.9916. R-squared values are calculated by squaring the correlation coefficient, and it describes how good the trendline fits the data points. An R^2 value of 1 has the best fit. The trendline for the pressure drop is therefore considered a good fit.

7.2   Odour Measurements

The first and second odour sample, paint and a blank sample, are consistently evaluated as the least detectable samples. This indicates that the first odour sample, which is paint, gave little to no noticeable odour. Paint is a viscous liquid which can explain why there is minimal off-gassing from the sample. The second odour sample is blank and should therefore have minimal detection. It has an average odour intensity of 1.25 on a scale from 0 to 6. Odour sample number 5 is also blank and has an average odour intensity of 1.97. This places the them between "very weak" and "weak" on the scale. Before the experiments started, it was a known fact that the test rig setup had some background odour coming from materials used in the construction. Some of the guesses for the two blank samples are perfume, cleaning product, liquorice, tobacco, nail polish remover or *something sweet*. These answers suggest that the background odour has a sweet, pungent and slightly chemical smell. Panel members are therefore asked to smell and familiarise themselves with the odour. This is to hopefully disregard this smell and focus on the new odours supplied to the system.

As presented in the results chapter, this is unfortunately not the case. Interestingly, the first blank sample is rated as more acceptable and less intense than the second blank sample. A possible reason for this is that the second blank sample is evaluated after the waffle odour. The odour may have lingered in the system and affected later samples. Preliminary testing was conducted to find out how long it takes for the odour to leave the system. One minute is given for the odour to leave the system, then an additional 30-seconds for the next sample to have time to disperse through the system. Therefore, sufficient time should have been given for the odour to disappear. Other factors may have come into play, like confusion due to background odour or still having the waffle smell fresh in mind.

The waffle odour may have been experienced as unsatisfactory for one of several reasons. It is the only odour sample that is hot, causing the particles to be lifted further into the system by the heated air. Therefore, the sample can reach a higher concentration, which is perceived as unacceptable over time by the panel members. In the questionnaire, the panel members are told to "Imagine you are exposed to this odour in your everyday life. How would you rate this odour on the following scale?". The idea of long term exposure to the odour may have caused them to rate it as less pleasant and less acceptable. It is also the only edible source with an odour that is typically thought of as pleasant. The human sense of smell aims to recognise potential food sources and can possibly have a lower odour threshold for the waffle sample.

How pleasant an odour is perceived is very individual. With the exception of the odour sample of the cleaning product and the waffle, all samples have an average hedonic tone value above 0 and are

considered pleasant. The waffle has an average hedonic tone of -0.75, but there is a large scatter in the rating from the panel members. They rate the odour between -4 and +3 on a scale going from -4 to +4. When comparing the charts for odour intensity and hedonic tone, a connection can be seen. The odour samples that score high on the odour intensity scale are also the samples rated as unpleasant by many panel members. This indicates a relationship between the intensity of the odour and the perceived hedonic tone.

It is difficult to establish the full extent of the cross-contamination through only the odour experiment. Therefore, the results should be compared to the formaldehyde and tracer gas experiment to establish a numerical size for the potential leakage and cross-contamination. However, considering that the membrane should stop the crossover of unwanted contaminants, the results indicate that the current membrane is not very selective towards odours in general.

7.3 Formaldehyde Measurements

The preliminary formaldehyde measurements show a considerable formaldehyde concentration in the basement before the experiment starts. The concentration is highest in the exhaust inlet air coming from the environmental chamber. This air represents the indoor air which usually has a 2 to 5 times higher VOC concentration than the outdoor air. The inlet supply air represents the clean outdoor air and has the lowest formaldehyde concentration at 1.8 times less than the supply air. Preferably there should be no traces of formaldehyde in the basement. However, the background concentration is in accordance with the normal relationship between indoor and outdoor VOC levels. The background concentration of formaldehyde should therefore not impact the results noticeably.

At times there is a quite large fluctuation in the measured formaldehyde concentration, as seen in figure 6.8, 6.9 and 6.10. This can be caused by an uneven release of formaldehyde from the particleboard. The formaldehyde is supplied by wetting the particleboard coated with a formaldehyde resin which releases particles. Unfortunately, it is impossible to guarantee that the conditions of the three experiments are identical. The same applies to the background concentration of formaldehyde in the basement where the experiment took place. The fluctuation in the measured concentration can also be affected by the placement of the VOC sensors. Because the sensors are quite large, they had to be placed some distance away from the exchanger core. This can have affected the measurements because it is likely that there are leaks along the pipes in the test rig. The air leakage test already established some internal and external leakages in the exchanger core. Therefore, the sensors' placement can have caused them to measure a lower formaldehyde level than what is present near the exchanger core.

The EATR is calculated both before and after the formaldehyde source is supplied to investigate the increase in concentration. This is necessary because there is a slight difference in the formaldehyde concentration at the start of the three experiments. The results show that the EATR and crossover are relatively high for the polypropylene membrane. It is also apparent that when the volumetric airflow rate increases, the cross-contamination decreases. A study by Huizing et al. (2015) investigated this phenomenon. They found that a high air change rate, achieved by increasing the volumetric airflow rate, can compensate for a high crossover. However, this will also reduce the energy-efficient and increase ventilation costs for the system. Due to technical problems with the VOC sensors, the crossover is calculated based on the preliminary measurements. Time delays at the lab made it impossible to repeat these measurements. Some caution should therefore be taken when comparing the EATR and crossover.

7.4 Air Leakage Measurements

The air leakage experiment investigates if the high cross-contamination can be caused by air leakages through the exchanger core. Results from the tracer gas test show a minimal internal and external air leakage at 1.67% and 3.60%, respectively. This contradicts the findings from the odour and formaldehyde experiments which indicates a large transfer through the membrane. The tracer gas experiment only measures the leakage through the exchanger core, while the odour and formaldehyde experiments use the whole test rig to conduct the measurements. There is a high probability of leakages in the pipe sections, especially in the connections between different sized pipes. However, this does not entirely explain the high cross-contamination found in the odour and formaldehyde experiments. A possible reason for the significant difference in measured leakage and cross-contamination is the membrane's selectivity to the different gases used in the experiment. This will be discussed further in subchapter 7.5.

The driving force for the heat exchange in the MEE is pressure differences. Air leakages are also caused by differences in pressure between the inside and outside of the system and between internal parts. The pressure drop through the heat exchanger was measured in the preliminary study and is presented in figure 6.2. Since the pressure drop increases as the volumetric airflow rate increases, it is logical to assume that the air leakage follows the same trend. However, air leakage measurements are only conducted at the highest volumetric airflow rate of the system as this is the standard method of air leakage testing.

7.5 Answers to Research Questions

1. Is the Perceived Air Quality Method the Best Method for Conducting Odour Experiments?

Odour analysis of air is normally performed using a sensorial, instrumental and/or mathematical method. This thesis investigates the odour using a sensorial method. However, an integrated approach combining senatorial and instrumental analysis of the air could have been beneficial. It could have given a more precise numerical understanding of the odour. Because the odour samples are common household products, it is difficult to supply them to the system at the same concentration. By using a combined technique like gas chromatography with olfactometry (GC-O) (see figure 2.1), the quantification of the odour could have been combined with the sensitivity of the human nose. Unfortunately, there is no gas chromatography equipment available at NTNU, and it is also quite expensive to purchase.

The sensorial method used in the thesis is the perceived air quality (PAQ) method. It is based on research conducted by Lars Gunnarsen and Per Ole Fanger in the '90s. The method was later standardised by ISO (ISO 16000-30:2014), and this is the approach used to conduct odour experiments in the thesis. Nineteen untrained students at NTNU are recruited to form the panel. They are subjected to five odour samples and two blank samples. Afterwards, they are asked to rate the samples based on the air acceptability, odour intensity and hedonic tone. At times the panel members rated the samples vastly different. Differences in how the air perceived from person to person are one of the weaknesses of the method. If a trained panel had been engaged, this could have been avoided. However, training or employing an already trained panel requires resources outside the scope of this thesis.

The difference in how the odour is perceived is assessed with an uncertainty analysis. Results from the analysis show that all samples are within the 90% confidence interval defined by ISO. However, if the

experiment were conducted with fewer participants, this accuracy target would probably not have been met. The presence of the background odour has probably interfered with the measurements, causing the need for more data points. The recommendation from ISO to conduct the experiment with 20 to 25 people should be followed even though the minimum requirement is 15 people. If the method established by ISO is followed, a sensorial investigation based on PAQ should be sufficient for assessing odour.

2. Has the odour experiment been influenced by the background odour in the test rig?

Most panel members were unable to guess the correct household odour source. Based on their guesses on the blank samples, it is reasonable to assume that the background odour has a sweet, pungent and slightly chemical smell. This odour would also have been present during the testing of the other sources. However, the experiment does not provide information on the extent to which the odours are affected. The chemical composition for the odour sources is quite different. Appendix G shows the products used in the odour experiment with pictures of the ingredient list. Since a gas chromatography analysis could not be conducted, the precise chemical composition is unknown. The waffle and food waste odour sources are made of organic materials, while the paint, cleaning product, perfume are inorganic materials made of solvents and alcohol. This difference in chemical structure can have affected the possibility of a fair and equal comparison of the results. Since the odour sources are made up of multiple and complex chemicals it is possible that certain substances transferred more easily through the membrane. This can have influenced the odour on the other side. Unlike the formaldehyde and tracer gas in research question 2, this potential selectivity is not quantifiable for the different odours with the chosen measurements method.

   Some of the odour samples has a higher odour intensity than the others. Because the initial odour concentration is unknown, it is difficult to know precisely why some samples are more noticeable than others. A theory is that there is a difference in the volatility of the samples. Samples with lower viscosity, i.e., cleaning spray and perfume, have lighter particles that are easily dispersed into the air. The same volatility is seen for the waffle sample due to the hot air created from the waffle iron. This causes them to reach a higher concentration in the air, making them distinguishable from the background odour. Based on the presented of evidence it is reasonable to assume that the odour experiment has been influenced by the background odour in the MEE test rig.

3. Are the Membranes Equally Selective in Relation to Different Vapours and Gases?

Results from the formaldehyde measurements showed high cross-contamination of VOCs through the membrane. Air leakage measurements using nitrous oxide indicated a relatively low internal and external leakage in the test rig. These results do not comply with the formaldehyde experiment. A reason can be that the membrane has a different selectivity towards the two different gases, i.e. formaldehyde and nitrous oxide.

   Table 7.1 shows a comparison of the chemical properties of formaldehyde and nitrous oxide, merged from table 3.6 and 3.8. The properties of nitrous oxide and formaldehyde are quite different. N_2O has a much lower boiling point which indicates it has a higher volatility than formaldehyde. The density is also considerably higher, meaning it has more particles per unit of volume. This affects the weight of the gas, which is 47% higher for the N_2O compared to the $HCHO$. Large gas molecules have a lower diffusion coefficient because they have difficulty penetrating the pores of the membrane. This causes the membrane to have a higher selectivity for large gas molecules. It can explain why the tracer gas experiment using N_2O

shows relatively small internal and external leakage. Formaldehyde gas molecules are smaller and can penetrate the membrane more easily, increasing the crossover in the exchanger core. The membrane's selectivity to formaldehyde can therefore be assumed to be lower than for nitrous oxide.

Table 7.1: Comparison of nitrous oxide and formaldehyde

	Molecular Weight [g/mol]	Boiling Point [$°C$]	Density [kg/m^3]
Formaldehyde, $HCHO$	30.026	-19.1	815
Nitrous oxide, N_2O	44.013	-88.5	1220

Another factor than can have affected the transfer of contaminants is the membranes attraction to certain chemicals over others. Through the research study it was discovered that the surface hydrophilicity is liked to the membranes ability to attract water molecules. Some contaminants, like formaldehyde, have a high water solubility which means it is easily dissolved in water. This could be a contributing factor to the selectivity of the membrane.

4. What is the Total Performance of the Membrane Energy Exchanger?

The total performance of the membrane is evaluated based on the physical properties of the membrane and the results from experiments conducted at the MEE test rig.

Table 4.3 in subchapter 4.3.1 shows the physical parameters for the polypropylene membrane investigated in the thesis. Conductive and convective heat transfer is affected by the membranes thickness, thermal conductivity and porosity, as established through the literature study on MEEs. There is no indication that effectiveness and potential cross-contamination is connected. However, the pores in porous membranes help increase the contact surfaces and, therefore, heat transfer. These pores could also reduce selectivity towards contaminants.

Table 7.2 summarises the results from the experiments conducted on the polypropylene membrane. The results are shown for the same volumetric airflow rate of 7.3 L/s. The sensible and latent effectiveness is quite high at 90% and 70%, respectively. ASHRAE defines the typical sensible effectiveness to be 55 - 75%, and the latent 25 - 60% (see table 3.1). This shows that the polypropylene membrane is quite permeable to heat and moisture. ASHRAE also defines a typical pressure drop through the MEE core to be between 100 and 500 Pa. The pressure drop ranges between 140 and 600 Pa for the different volumetric airflow rates investigated at the test rig. This indicates that the pressure drop is somewhat high through the MEE core. Previous research indicates that a large contributor to increased pressure drop is the internal spacer in the MEE core. However, the spacers are important to ensure that the membranes do not collapse or stick together. It also helps to increase the heat and mass transfer.

Table 7.2: Summary of the results conducted on the polypropylene membrane, at a volumetric airflow rate of 7.3 L/s.

Parameter	Result
Latent effectiveness, [-]	0.9
Sensible effectiveness, [-]	0.7
Pressure drop, [Pa]	575
EATR$_{HCHO}$, [%]	46.5
Crossover$_{HCHO}$ [%]	62.9

The formaldehyde experiments measured the VOC transfer through the membrane. Results indicated that the membrane is not very selective towards formaldehyde. The exhaust air transfer rate and crossover are measured to be 46.6% and 62.9%, respectively. ASHRAE defines the typical EATR for MEEs to be between 0 and 5%. The crossover is also extremely high. In a literature study conducted by Huizing et al. (2015), the authors found that at a moderate crossover of 15%, the contaminants would have a minimal impact on the indoor air quality under standard conditions. With a crossover four times higher, the impact cannot be assumed to be minimal any longer. The crossover of formaldehyde is even higher for measurements conducted at lower volumetric airflow rates. However, the air leakage test using nitrous oxide indicated a low internal and external leakage. Therefore, it is plausible that the membrane is more selective towards some gases, but more experiments need to be conducted to conclude further.

The odour measurements also indicate large cross-contamination through the polypropylene membrane. Most of the odour samples have lower air acceptability and higher odour intensity than the blank samples used for reference. Common for the most noticeable odour samples is that they have higher volatility which helps them disperse into the air at a higher concentration. Considering that the membrane should stop all odour sources from transferring through the membrane, it can be assumed that the current membrane is not very selective towards odours.

The polypropylene membrane has a high effectiveness, but the protection against crossover of contaminants is inadequate. Therefore, the total performance is considered to be low.

Chapter 8

Conclusion

A quasi-counter flow membrane energy exchanger has been experimentally investigated in order to establish the total performance. This includes the sensible and latent effectiveness, pressure drop and cross-contamination. The cross-contamination through the membrane was tested by measuring the crossover of volatile organic compounds and odours

Results show that the membrane energy exchanger reaches a high sensible and latent effectiveness, averaging at 90% and 70%, respectively. The pressure drop increased from 140 to 600 Pa when the volumetric airflow rate is varied between 3 and 7.7 L/s during the experiment. This is considered to be slightly high for an exchanger of this type. The VOC transfer is measured using formaldehyde and results shows that the exhaust air transfer ratio averages at 44.67% when the airflow rate is 7.3 L/s and has increased to 65.72% when the airflow rate is 4.2 L/s. The same is seen for the crossover, where it increases from 62.93% to 81.29% when the airflow rate decreases. However, these measurements indicate a large cross-contamination through the membrane. This is supported by the odour experiment. The odour measurement is carried out using the perceived air quality method and 19 panels members who evaluate the ventilation air. Most panel members evaluate the average air acceptability for the two blank odour samples to be higher than for the household odour sources. The two blank samples used for comparison are evaluated to have a higher average air acceptability than the household odour sources by 64% and 78% of the panel members, respectively. The odour intensity is rated to be lower for these samples by 63% of the panel members for the first blank sample and by 50% for the second. This indicates that there is a cross-contamination between the exhaust and supply side of the MEE.

An air leakage measurement is conducted to investigate if the cross-contamination is caused by poor airtightness in the exchanger core. The test found that the internal leakage is 1.67% and the external leakage is 3.57%. This disproves the theory of poor airtightness. Another plausible answer is that the polypropylene membrane has different selectivity towards different vapours and gases.

Based on these results the total performance of the polypropylene membrane is evaluated to be high in relation to heat transfer, but low in relation to cross-contamination. This raises questions about how suitable the membrane is for use in building types that have special requirements for ventilation. Additional porous membrane materials should be investigated to see if this is a trend among porous membranes.

Chapter 9

Future Work

Dense membranes where the norm in membrane energy exchangers for a long time. In recent years porous membranes have been investigated because they have shown great heat transfer properties. The results from this thesis indicate a problem with crossover of VOCs and odour in MEEs using these membranes.

Due to time delays during the construction and experimental work, the two additional membrane materials could not be investigated. Testing them could have provided insightful information about the crossover of contaminants in porous membrane materials. Further research should therefore investigate more membrane materials to compare and conclude on the total performance of these membranes.

Another relevant research objective would be to investigate if any actions can be taken to reduce the cross-contamination. This could include changes to the geometry of the MEE core, or changes to the ventilation system as a whole.

Bibliography

Albdoor, A. K., Z. Ma, and P. Cooper (2019). "Moisture diffusion measurement and evaluation for porous membranes used in enthalpy exchangers". In: Energy Procedia 160, pp. 499–506.

— (2020). "Experimental investigation and performance evaluation of a mixed-flow air to air membrane enthalpy exchanger with different configurations". In: Applied Thermal Engineering 166.

Albdoor, A. K., Z. Ma, P. Cooper, et al. (2021). "Air-to-air enthalpy exchangers: Membrane modification using metal-organic frameworks, characterisation and performance assessment". In: Journal of Cleaner Production 293.

Anand, S.S., B. K. Philip, and H.M. Mehendale (2014). Encyclopedia of Toxicology. 3rd. Oxford: Academic Press, pp. 967–970.

Andrew Dravnieks, A., T. Masurat, and R. A. Lamm (1984). "Hedonics of Odors and Odor Descriptors". In: Journal of the Air Pollution Control Association 34, pp. 752–755.

ASHRAE, The American Society of Heating, Refrigerating and Air-Conditioning Engineers (2016). ASHRAE Handbook - Heating, Ventilating and Air-Conditioning Systems ans Equipment. Handbook. Georgia, USA.

Attramadal, T., P. Schwarze, and R. Becher (2015). Anbefalte faglige normer for inneklima. Tech. rep. Oslo, NO: Nasjonalt folkehelseinstitutt.

Bax, C., S. Sironi, and L. Capell (2020). "How Can Odors Be Measures? An Overview of Methods and Their Applications". In: Atmosphere 11, p. 92.

Biotechnology Information, National Center for (2021). PubChem Compound Summary for CID 263, 1-Butanol. Accessed 25.01.2021. URL: https://pubchem.ncbi.nlm.nih.gov/compound/1-Butanol.

Cengel, Y.A. and J.M. Cimbala (2014). Fluid Mechanics: Fundamentals and Applications. Mcgraw Hill, pp. 1–74, 347–419.

Conti, C., M. Guarino, and J. Bacenetti (2020). "Measurements Techniques and Models to Assess Odor Annoyance: A Review". In: Environment International 134.

DiBK (2017). Byggteknisk forskrift (TEK17). Tech. rep. Oslo: Direktoratet for byggkvalitet.

Gram, O. K. (2019). Use of low cost pollutant sensors for developing healthy demand controlled ventilation strategies. Master's Thesis. Trondheim, NO: NTNU.

Gunnarsen, L. and P. O. Fanger (1992). "Adaption to Indoor Air Pollution". In:
    Environmental International 18, pp. 43–54.

Huizing, R., H. Chen, and F. Wong (2015). "Contaminant Transport in Membrane Based Energy
    Recovery Ventilators". In: Science and Technology for the Built Environment 21, pp. 54–66.

Hyttinen, M. et al. (2007). "Odors and volatile organic compounds released from ventilation
    filters". In: Atmospheric Environment 41, pp. 4029–4039.

ISO, International Organization for Standardization. (2014).
    Indoor air — Part 30: Sensory testing of indoor air (ISO 16000-30:2014). Standard. Geneva,
    Switzerland.

Kays, W. M., R. K. Jain, and S. Sabherwal (1968). "The effectiveness of a counter-flow heat
    exchanger with cross-flow headers". In: International Journal of Heat and Mass Transfer 11,
    pp. 772–774.

Kays, W. M. and A. L. London (1984). Compact Heat Exchangers. 3rd. Mcgraw-Hill.

Koester, S. et al. (2016). "Spacer enhanced heat and mass transfer in membrane-based enthalpy
    exchangers". In: Journal of Membrane Science 520, pp. 566–573.

Kolarik, J. et al. (2014). "Field measurements of perceived air quality and concentration of volatile
    organic compounds in four offices of the university building". In:
    Indoor and Built Environment 24, pp. 1048–1058.

Kraus, M. and I. J. Senitkova (2019). "A Study of Perceived Air Quality and Odours". In:
    Materials Science and Engineering 471.

Laussmann, D. and D. Helm (2011).
    Chemistry, Emission Control, Radioactive Pollution and Indoor Air Quality. Accessed
    06.05.2021. Rijeka, Croatia: Elsevier, pp. 365–406. URL:
    https://www.intechopen.com/books/chemistry-emission-control-radioactive-
    pollution-and-indoor-air-quality/air-change-measurements-using-tracer-gases-
    methods-and-results-significance-of-air-change-for-indoor.

Lecomte-Saur, S. (2020).
    Measurements and analysis of membrane heat exchanger for energy efficient ventilation.
    Master's Thesis. Trondheim, NO: NTNU.

Leonardos, G., D. Kendall, and N. Barnard (1969). "Odor Threshold Determinations of 53 Odorant
    Chemicals". In: Journal of the Air Pollution Control Association 19, pp. 91–95.

Lewkowska, P. et al. (2016). "The Use of Sensory Analysis Techniques to Assess the Quality of
    Indoor Air". In: Critical Reviews in Analytical Chemistry 47, pp. 37–51.

Liu, P. et al. (2016). "Performance of a Quasi-Counter-Flow Air-to-Air Membrane Energy
    Exchanger in Cold Climates". In: Energy and Buildings 119, pp. 129–142.

— (2017). "Energy Transfer and Energy Saving Potentials of Air-to-Air Membrane Energy
    Exchanger for Ventilation in Cold Climates". In: Energy and Buildings 135, pp. 95–108.

McAllister, E. W. (2014).
    A Manual of Quick, Accurate Solutions to Everyday Pipeline Engineering Problems. 8th.
    Amsterdam: Elsevier.

Mentese, S. et al. (2020). "A long-term multi-parametric monitoring study: Indoor air quality
     (IAQ) and the sources of the pollutants, prevalence of sick building syndrome (SBS)
     symptoms, and respiratory health indicators". In: Atmospheric Pollution Research.

Min, J. and M. Su (2011). "Performance Analysis of a Membrane-Based Energy Recovery
     Ventilator: Effects of Outdoor Air State". In: Applied Thermal Engineering 31, pp. 4036–4043.

Ministry of Labour and Social Affairs (2011). Forskrift om tiltaks- og grenseverdier. Tech. rep.
     Accessed 27.04.2021. Oslo, NO: Arbeidstilsynet. URL:
     https://www.arbeidstilsynet.no/regelverk/forskrifter/forskrift-om-tiltaks--og-
     grenseverdier/.

Niu, J.L. and L.Z. Zhang (2001). "Membrane-based Enthalpy Exchanger: material considerations
     and clarification of moisture resistance". In: Journal of Membrane Science 189, pp. 179–191.

Novakovic, V. et al. (2007). ENØK i bygninger: effektiv energibruk. 3rd. Oslo: Gyldendal
     undervisning, pp. 376–380.

NS, Standard Norge (2011).
     Performance testing of components/products for residential ventilation (NS-EN 13141-7:2010).
     Standard. Oslo, Norway.

Patel, H. et al. (2013). "Contaminant transfer in run-around membrane energy exchangers". In:
     Energy and Buildings 70, pp. 94–105.

Peng, L. (2016).
     Energy Recovery with Air-to-air Membrane Energy Exchanger for Ventilation in Cold Climates.
     Doctoral Thesis. Trondheim, NO: NTNU.

Rafati Nasr, M. et al. (2014). "A review of Frosting in Air-to-Air Energy Exchangers". In:
     Renewable and Sustainable Energy Reviews 30, pp. 538–554.

Rapp, B. E. (2017). Microfluidics: Modelling, Mechanics and Mathematics. Oxford: Elsevier,
     pp. 243–263.

Rashidi, S. et al. (2019). "Potentials of porous materials for energy management in heat
     exchangers – A comprehensive review". In: Applied Energy 243, pp. 206–232.

Sarigiannis, D. A. (2014).
     Combined or multiple exposure to health stressors in indoor built environments. Tech. rep.
     Copenhagen: World Health Organization.

Senitkova, I. J. and M. Kraus (2018). "Indoor TVOC and Odor Pollution - Chemical and Sensory
     Assessment Using the Glass Test Chamber". In: Journal of Heat and Mass Transfer 15,
     pp. 653–673.

Shah, R.K. and D.P. Sekulic (2003). Fundamentals of Heat Exchanger Design. Mcgraw Hill,
     pp. 378–420.

Sherman, M.H. (n.d.). "Tracer-Gas Techniques for Measuring Ventilation in a Single Zone". In:
     Building and Environment 25 (), pp. 365–374.

Siegele, D. and F. Ochs (2019). "Effectiveness of a membrane enthalpy heat exchanger". In:
     Applied Thermal Engineering 160.

Stauffer, E., J. A. Dolan, and R. Newman (2008). Fire Debris Analysis. Burlington: Academic Press,
     pp. 235–293.

US EPA (2014). Technical Overview of Volatile Organic Compounds. Accessed 19.02.2021. URL:
https://www.epa.gov/indoor-air-quality-iaq/technical-overview-volatile-organic-compounds.

US EPA, United States Environmental Protection Agency. (2018).
Volatile Organic Compounds' Impact on Indoor Air Quality. Accessed 21.09.2020. URL:
https://www.epa.gov/indoor-air-quality-iaq/volatile-organic-compounds-impact-indoor-air-quality.

WHO, World Health Organization. (2010).
WHO guidelines for indoor air quality : selected pollutants. Tech. rep. Copenhagen, DEN:
WHO, pp. 103–142.

— (2011). Agents Classified by the IARC Monographs, Volumes 1–128. Accessed 24.02.2021.
URL: https://monographs.iarc.who.int/agents-classified-by-the-iarc/.

Woods, J. (2014). "Membrane processes for heating, ventilation, and air conditioning". In:
Renewable and Sustainable Energy Reviews 33, pp. 290–304.

Zhang, L.Z. (2008). Total heat recovery : heat and moisture recovery from ventilation air. Nova
Science Publishers, pp. 131–154.

— (2010). "Heat and Mass Transfer in a Quasi-Counter Flow Membrane-Based Total Heat
Exchanger". In: International Journal of Heat and Mass Transfer 53, pp. 23–24.

— (2012). "Progress on Heat and Moisture Recovery with Membranes: From Fundamentals to
Engineering Applications". In: Energy Conversion and Management 63, pp. 173–195.

— (2014). Conjugate Heat and Mass Transfer in Heat Mass Exchanger Ducts. Elsevier Academic
Press, pp. 1–20, 93–124, 670–706.

Zhang, L.Z. and Y. Jiang (1999). "Heat and Mass Transfer in a Membrane-Based Energy Recovery
Ventilator". In: Journal of Membrane Science 163, pp. 29–38.

Zhang, Q. et al. (2002). "Correlation between odour intensity assessed by human assessors and
odour concentration measured with olfactometers". In: Canadian Biosystems Engineering 144,
6.27–6.32.

Calculation of Volumetric Airflow Rate

The volumetric flow rate in the MEE test rig is calculated based on the pressure difference on either side on the orifice plates in the channel. The pressure difference in given in Pascal, Pa, and needs to be converted to volumetric air flow, L/s, afterwards. This is done with the help of an Excel sheet based on the standards NS-EN ISO 5167-1 and NS-EN ISO 5167-2.

The parameters necessary to do the calculation is provided in table A.1. Air density is given by the temperature, and at $20°C$ the density is 1.2041 kg/m^3.

Table A.1: Parameters used to calculate the volumetric flow rate from the pressure over the orifice plates in the MEE test rig

Parameter	Value
Diameter of duct [mm]	100
Diameter of orifice plate [mm]	45
Diameter ratio [-]	0.45
Dynamic viscosity of air at 293 K [Ns/m^2]	$1.79 \cdot 10^{-5}$
Kinematic viscosity of air at 293 K [m^2/s]	$1.45 \cdot 10^{-5}$

The volumetric air flow rate for the test rig experiments done at room temperature ($20°C$) is shown in table A.2.

Table A.2: Volumetric air flow rate for the MEE test rig at $20°C$

Pressure drop [Pa]	Volumetric air flow rate [L/s]
10	4.2
21	6
32	7.3

Appendix B

Odour Experiment Questionnaire

The odour questionnaire is printed as a brochure on one sheet of A4 paper.

Odour experiment on the MEE test rig

<u>To qualify as a panellist, you should:</u>

- Be motivated and available to complete the experiment.
- Have no health conditions or allergies which could affect the sense of smell.
- Avoid using personal hygiene products containing perfume.
- Ideally not smoke or use tobacco, however they can participate is they refrain from tobacco two hours before and during the experiment.
- Not eat, chew gum or drink anything except water during the last 30 minutes before the experiments.

Personal information: (You do not have to fill in the personal information if you feel uncomfortable doing so)

Age: _____

Gender: _____

Do you suffer from a disease or allergy which affect the sense of smell? (Yes/No) _____

Do you smoke? (Yes/No) _____

Do you use "snus"? (Yes/No) _____

Have you consumed any food/ beverage in the last 30 minutes? (not including water, Yes/No) _____

IMPORTANT!

The odour you are set to evaluate is the odour that is different from the background odour of the system.

Do NOT discuss your opinion about the odour with the other participants during the experiment as this can influence your opinion.

Thank you for participating!

Air acceptability:

1. Imagine you are exposed to this odour in your everyday life. Would you consider this odour acceptable? (Yes or No)

	Test 1	Test 2	Test 3	Test 4	Test 5	Test 6	Test 7
Yes or No?							

2. Imagine you are exposed to this odour in your everyday life. How would you rate this odour on the following scale?

+1 ——— Clearly acceptable

Just acceptable
0 ———
Just not acceptable

-1 ——— Clearly not acceptable

Test 1	Test 2	Test 3	Test 4	Test 5	Test 6	Test 7
+1 — 0 — -1 —	+1 — 0 — -1 —	+1 — 0 — -1 —	+1 — 0 — -1 —	+1 — 0 — -1 —	+1 — 0 — -1 —	+1 — 0 — -1 —

Odour intensity:

How do you experience the intensity of the odour on the following scale?

0	No odour
1	Very weak
2	Weak
3	Distinct
4	Strong
5	Very strong
6	Extremely strong
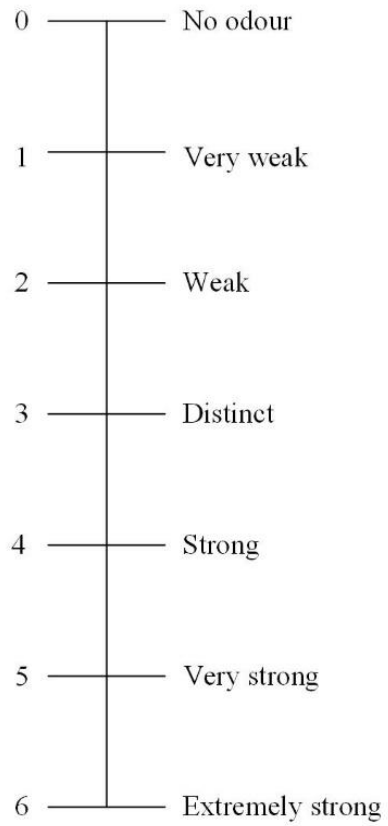
Test 1	Test 2	Test 3	Test 4	Test 5	Test 6	Test 7
0	0	0	0	0	0	0
1	1	1	1	1	1	1
2	2	2	2	2	2	2
3	3	3	3	3	3	3
4	4	4	4	4	4	4
5	5	5	5	5	5	5
6	6	6	6	6	6	6

Hedonic tone:

How pleasant or unpleasant to you experience the odour? Rate it on the scale below.

Test 1	Extremely unpleasant ···-4···-3···-2···-1···0···1···2···3···4··· Very pleasant
Test 2	Extremely unpleasant ···-4···-3···-2···-1···0···1···2···3···4··· Very pleasant
Test 3	Extremely unpleasant ···-4···-3···-2···-1···0···1···2···3···4··· Very pleasant
Test 4	Extremely unpleasant ···-4···-3···-2···-1···0···1···2···3···4··· Very pleasant
Test 5	Extremely unpleasant ···-4···-3···-2···-1···0···1···2···3···4··· Very pleasant
Test 6	Extremely unpleasant ···-4···-3···-2···-1···0···1···2···3···4··· Very pleasant
Test 7	Extremely unpleasant ···-4···-3···-2···-1···0···1···2···3···4··· Very pleasant

Odour:

Which odour do you think you were subjected to? Make a guess below.

PS: They are all common odours to find at home.

Test 1	
Test 2	
Test 3	
Test 4	
Test 5	
Test 6	
Test 7	

Sketches for the MEE Construction
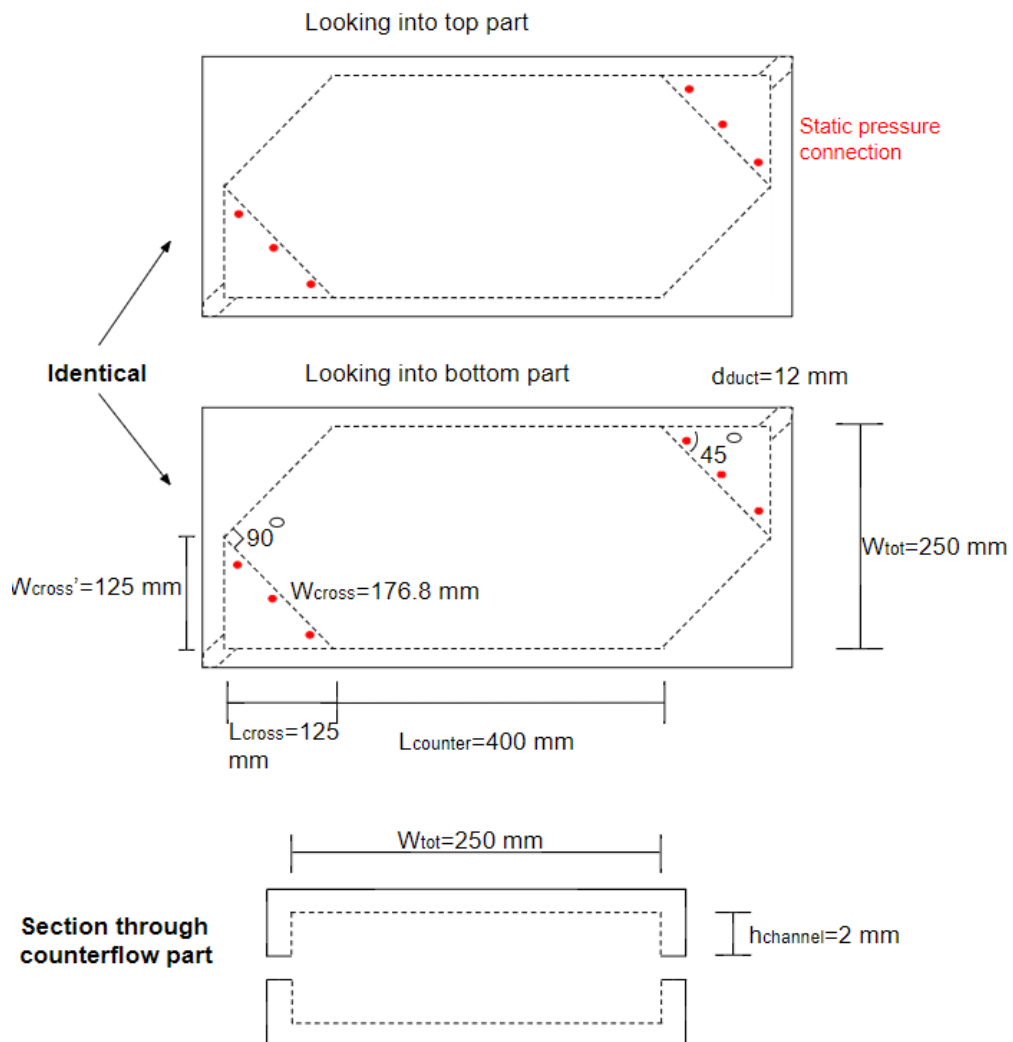

Figure C.1: Sketch for the construction of lexan pieces for the MEE core

Appendix D

Formaldehyde Measurements
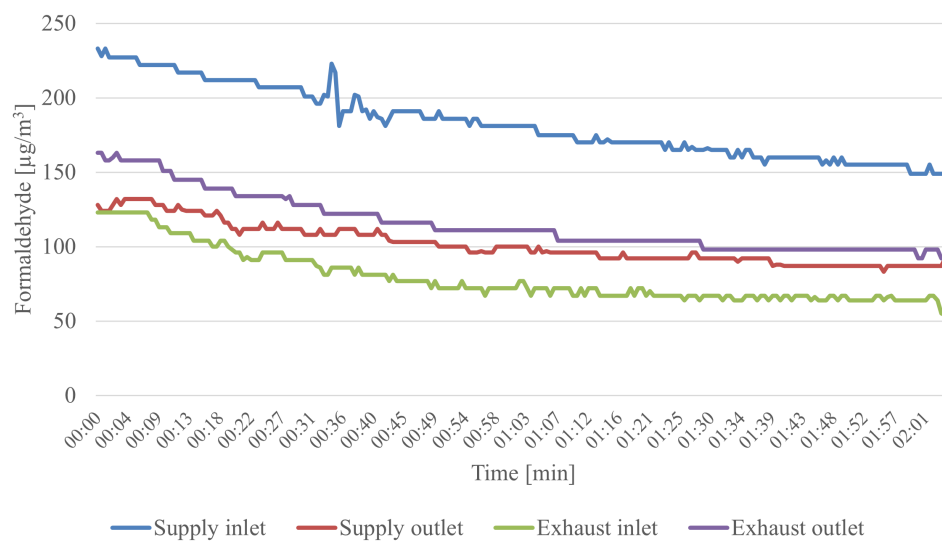
D.1 Volumetric Airflow Rate at 7.3 L/s

Figure D.1: High airflow, second experiment
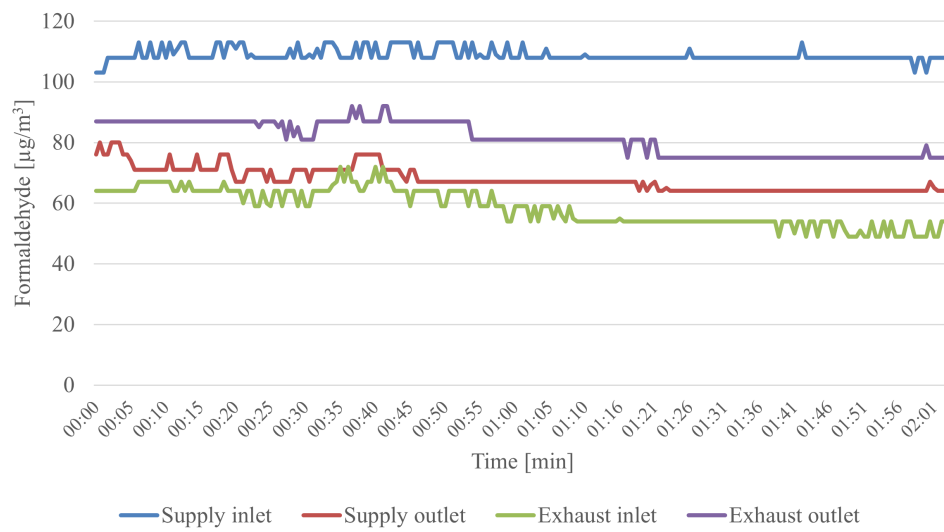
D.2   Volumetric Airflow Rate at 6 L/s

Figure D.2: Medium airflow, second experiment
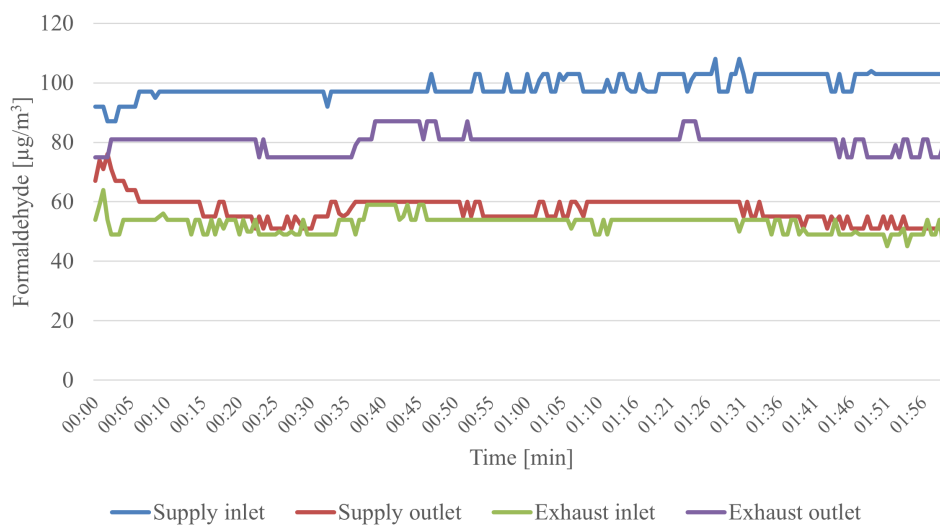
D.3   Volumetric Airflow Rate at 4.3 L/s

Figure D.3: Low airflow, second experiment

Risk Assessment

NTNU [image] HSE	Hazardous activity identification process	Prepared by	Number	Date
		HSE section	HMSRV2601E	09.01.2013
		Approved by		Replaces
		The Rector		01.12.2006

Unit: *EPT*   **Date: 08.06.2021**

Line manager:

Participants in the identification process (including their function)**:**

Short description of the main activity/main process: Master project for student Mariell Skaten. Measurements and analysis of membrane heat exchanger for energy efficient ventilation.

Is the project work purely theoretical? (YES/NO): NO   *Answer "YES" implies that supervisor is assured that no activities requiring risk assessment are involved in the work. If YES, briefly describe the activities below. The risk assessment form need not be filled out.*

Signatures: *Responsible supervisor:* [signature]   *Student:* [signature]

ID nr.	Activity/process	Responsible person	Existing documentation	Existing safety measures	Laws, regulations etc.	Comment
01	Running effectiveness experiments at the membrane energy exchanger test rig	Mariell Skaten	NO	NO	NO	
02	Running VOC and odour experiments at the membrane energy exchanger test rig	Mariell Skaten	NO	NO	NO	

			Prepared by	Number	Date	
NTNU	**Risk assessment**		HSE section	HMSRV2603E	04.02.2011	
HSE/KS			Approved by		Replaces	
			The Rector		01.12.2006	

Unit: *EPT*   **Date: 08.06.2021**

Line manager:

Participants in the identification process (including their function)**:**

Short description of the main activity/main process: Master project for student Mariell Skaten. Measurements and analysis of membrane heat exchanger for energy efficient ventilation.

Signatures: *Responsible supervisor:*   *Student:*

Activity from the identification process form	Potential undesirable incident/strain	Likelihood: Likelihood (1-5)	Consequence: Human (A-E)	Environment (A-E)	Economy/ material (A-E)	Risk Value (human)	Comments/status Suggested measures
01 and 02	Noise from fans at the test rig.	4	A	A	A	A4	Wear hearing protection if the noise is perceived as annoying.
02	Annoying odour from the odour samples spreading.	4	A	A	A	A4	Try to ventilate the premises.

Likelihood, e.g.:
1. *Minimal*
2. *Low*

Consequence, e.g.:
A. *Safe*
B. *Relatively safe*

Risk value (each one to be estimated separately):
Human = Likelihood x Human Consequence
Environmental = Likelihood x Environmental consequence

3.	Medium	C.	Dangerous
4.	High	D.	Critical
5.	Very high	E.	Very critical

Financial/material = Likelihood x Consequence for Economy/materiel

Potential undesirable incident/strain

Identify possible incidents and conditions that may lead to situations that pose a hazard to people, the environment and any materiel/equipment involved.

Criteria for the assessment of likelihood and consequence in relation to fieldwork

Each activity is assessed according to a worst-case scenario. Likelihood and consequence are to be assessed separately for each potential undesirable incident. Before starting on the quantification, the participants should agree what they understand by the assessment criteria:

Likelihood

Minimal 1	Low 2	Medium 3	High 4	Very high 5
Once every 50 years or less	Once every 10 years or less	Once a year or less	Once a month or less	Once a week

Consequence

Grading	Human	Environment	Financial/material
E **Very critical**	May produce fatality/ies	Very prolonged, non-reversible damage	Shutdown of work >1 year.
D **Critical**	Permanent injury, may produce serious serious health damage/sickness	Prolonged damage. Long recovery time.	Shutdown of work 0.5-1 year.
C **Dangerous**	Serious personal injury	Minor damage. Long recovery time	Shutdown of work < 1 month
B **Relatively safe**	Injury that requires medical treatment	Minor damage. Short recovery time	Shutdown of work < 1week
A **Safe**	Injury that requires first aid	Insignificant damage. Short recovery time	Shutdown of work < 1day

The unit makes its own decision as to whether opting to fill in or not consequences for economy/materiel, for example if the unit is going to use particularly valuable equipment. It is up to the individual unit to choose the assessment criteria for this column.

NTNU		Risk assessment	Prepared by	Number	Date	
			HSE section	HMSRV2603E	04.02.2011	
			Approved by		Replaces	
HSE/KS			The Rector		01.12.2006	

Risk = Likelihood x Consequence
Please calculate the risk value for "Human", "Environment" and, if chosen, "Economy/materiel", separately.

About the column "Comments/status, suggested preventative and corrective measures":
Measures can impact on both likelihood and consequences. Prioritise measures that can prevent the incident from occurring; in other words, likelihood-reducing measures are to be prioritised above greater emergency preparedness, i.e. consequence-reducing measures.

NTNU		Risk matrix	prepared by	Number	Date	
⬛			HSE Section	HMSRV2604	8 March 2010	
HSE/KS			approved by	Page	Replaces	
			Rector	4 of 4	9 February 2010	

MATRIX FOR RISK ASSESSMENTS at NTNU

CONSEQUENCE	Extremely serious	E1	E2	E3	E4	E5
	Serious	D1	D2	D3	D4	D5
	Moderate	C1	C2	C3	C4	C5
	Minor	B1	B2	B3	B4	B5
	Not significant	A1	A2	A3	A4	A5
		Very low	Low	Medium	High	Very high
		LIKELIHOOD				

Principle for acceptance criteria. Explanation of the colours used in the risk matrix.

Colour		Description
Red		Unacceptable risk. Measures must be taken to reduce the risk.
Yellow		Assessment range. Measures must be considered.
Green		Acceptable risk Measures can be considered based on other considerations.

Appendix F

Uncertainties

F.1 Direct measurements

Systematic error: U_s, Given by the manufacturer. For the measurement devices used on the test rig (temperature, relative humidity and pressure drop), table 4.1 shows the systematic error provided by the manufacturers.

Random error: $U_R = \pm \dfrac{s}{\sqrt{n}}$

       Where:

$$\overline{x} = \frac{\sum x}{n}$$

$$s = \sqrt{\frac{\sum (x - \overline{x})^2}{n-1}}$$

Resulting error: $\Delta U = \pm \sqrt{U_R^2 + U_S^2}$

Table F.1 shows the uncertainties for the direct measurements.

Table F.1: The uncertainties for the direct measurements, conducted at the highest volumetric airflow rate at the test rig, 7.2 L/s.

Parameter	Uncertainty
T_{si} [4°C]	± 0.03 @ 15.40
T_{so} [°C]	± 0.03 @ 21.17
T_{ei} [°C]	± 0.04 @ 21.86
T_{eo} [°C]	± 0.02 @ 16.36
RH_{si} [%]	± 0.35 @ 31.32
RH_{so} [%]	± 0.23 @ 33.27
RH_{ei} [%]	± 0.42 @ 36.19
RH_{eo}[%]	± 0.28 @ 36.29
Pressure drop [Pa]	± 4.95 @ 588.50
$HCHO_{si}$ [$\mu g/m^3$]	± 21.50 @ 116.48
$HCHO_{so}$ [$\mu g/m^3$]	± 5.58 @ 84.50
$HCHO_{ei}$ [$\mu g/m^3$]	± 3.69 @ 54.49
N_2O_{si} [PPM]	± 0.75 @ 7.82
N_2O_{so} [PPM]	± 0.65 @ 8.20
N_2O_{ei} [PPM]	± 1.44 @ 25.95
N_2O_{eo} [PPM]	± 0.79 @ 25.47

F.2 Indirect measurements

Indirect measurements are parameters which rely on multiple variables to be measured. For example; the moisture content in the air is dependent on both the relative humidity and the temperature of the air to be found. Below the formulas for the resulting error in moisture content and sensible and latent effectiveness measurements is shown. Table F.2 shows the uncertainties for the indirect measurements.

Table F.2: The uncertainties for the indirect measurements, conducted at the highest volumetric airflow rate at the test rig, 7.2 L/s.

Parameter	Uncertainty
$w_{si}[kg/kg]$	± 0.000035 @ 0.003350
$w_{so}[kg/kg]$	± 0.000037 @ 0.005143
$w_{ei}[kg/kg]$	± 0.000073 @ 0.005843
$\epsilon_{sensible}[\%]$	± 0.08 @ 89.27
$\epsilon_{latent}[\%]$	± 2.22 @ 71.98

F.2.1 Moisture Content

$$w = \frac{RH \cdot 10^7}{6.462 exp(\frac{5419}{T})}$$

$$\Delta w = \pm \sqrt{\left(\frac{\partial w}{\partial RH} \cdot \Delta RH\right)^2 + \left(\frac{\partial w}{\partial T} \cdot \Delta T\right)^2}$$

$$\Delta w = \pm \sqrt{\left(\frac{RH \cdot 10^7}{6.462exp(\frac{5419}{T})}\right)^2 + \left(\frac{5418}{T^2}w \cdot \Delta T\right)^2}$$

F.2.2 Sensible and Latent Effectiveness

$$\epsilon_S = \frac{t_{so} - t_{si}}{t_{ei} - t_{si}}$$

$$\epsilon_L = \frac{w_{so} - w_{si}}{w_{ei} - w_{si}}$$

$$\Delta \epsilon_S = \pm \sqrt{\left(\frac{\partial \epsilon_S}{\partial T_{so}} \cdot \Delta T_{so}\right)^2 + \left(\frac{\partial \epsilon_S}{\partial T_{ei}} \cdot \Delta T_{ei}\right)^2 + \left(\frac{\partial \epsilon_S}{\partial T_{si}} \cdot \Delta T_{si}\right)^2}$$

$$\Delta \epsilon_S = \pm \sqrt{\left(\frac{1}{t_{ei} - t_{si}}\Delta T_{so}\right)^2 + \left(\frac{T_{si} - T_{so}}{(t_{ei} - t_{si})^2}\Delta T_{ei}\right)^2 + \left(\frac{T_{so} - T_{ei}}{(t_{ei} - t_{si})^2}\Delta T_{si}\right)^2}$$

The equations for latent effectiveness have the same setup, but uses the moisture content, w, instead of temperature, t.

F.3 Uncertainty of the Sensory Assessments

The equations used to calculate the uncertainty in the sensory assessments is shown in subchapter 5.6.3.

Table F.3 shows the t-distribution for different confidence intervals and degrees of freedom. The degree of freedom is calculated as $n - 1$, where n is the number of participants.

Table F.3: t-Distribution for different confidence interval percentiles and degrees of freedom.

n-1	$t_{.5}$	$t_{.75}$	$t_{.80}$	$t_{.85}$	$t_{.90}$	$t_{.95}$	$t_{.975}$	$t_{.99}$	$t_{.995}$	$t_{.999}$	$t_{.9995}$
10	0.000	0.700	0.879	1.093	1.372	1.812	2.228	2.764	3.169	4.144	4.587
11	0.000	0.697	0.876	1.088	1.363	1.796	2.201	2.718	3.106	4.025	4.437
12	0.000	0.695	0.873	1.083	1.356	1.782	2.179	2.681	3.055	3.930	4.318
13	0.000	0.694	0.870	1.079	1.350	1.771	2.160	2.650	3.012	3.852	4.221
14	0.000	0.692	0.868	1.076	1.345	1.761	2.145	2.624	2.977	3.787	4.140
15	0.000	0.691	0.866	1.074	1.341	1.753	2.131	2.602	2.947	3.733	4.073
16	0.000	0.690	0.865	1.071	1.337	1.746	2.120	2.583	2.921	3.686	4.015
17	0.000	0.689	0.863	1.069	1.333	1.740	2.110	2.567	2.898	3.646	3.965
18	0.000	0.688	0.862	1.067	1.330	1.734	2.101	2.552	2.878	3.610	3.922
19	0.000	0.688	0.861	1.066	1.328	1.729	2.093	2.539	2.861	3.579	3.883
20	0.000	0.687	0.860	1.064	1.325	1.725	2.086	2.528	2.845	3.552	3.850

With 19 panel members in the odour experiment, the t-distribution is 1.734.

Odour Samples

Figure G.1: Odour sample 1 - Paint

Figure G.2: Odour sample 3 - Cleaning spray

Figure G.3: Odour sample 4 - Waffle mix

Figure G.4: Odour sample 6 - Perfume

Figure G.5: Odour sample 7 - Food waste. *non copyrighted picture from www.pexels.com*